Thermal Performance of 69 kV Underground Cables

by

Tong Wang

A Thesis Presented in Partial Fulfillment
of the Requirements for the Degree
Master of Science

Approved November 2013 by the
Graduate Supervisory Committee:

Daniel Tylavsky, Chair
Keith Holbert
George Karady

ARIZONA STATE UNIVERSITY

December 2013

ABSTRACT

Underground cables have been widely used in big cities. This is because underground cables offer the benefits of reducing visual impact and the disturbance caused by bad weather (wind, ice, snow, and the lightning strikes). Additionally, when placing power lines underground, the maintenance costs can also be reduced as a result.

The underground cable rating calculation is the most critical part of designing the cable construction and cable installation. In this thesis, three contributions regarding the cable ampacity study have been made. First, an analytical method for rating of underground cables has been presented. Second, this research also develops the steady state and transient ratings for Salt River Project (SRP) 69 kV underground system using the commercial software CYMCAP for several typical substations. Third, to find an alternative way to predict the cable ratings, three regression models have been built. The residual plot and mean square error for the three methods have been analyzed. The conclusion is dawn that the nonlinear regression model provides the sufficient accuracy of the cable rating prediction for SRP's typical installation.

ACKNOWLEGEMENT

I would like to first and foremost thank my advisor, Dr. Daniel Tylavsky, for his encouragement, guidance, and support on this research work. In the meantime, I appreciate Salt River Project offered me an opportunity to conduct a research on their 69 kV underground systems. During the course of the project, Jim Hunt, Bryce Priest, and Catherine O'Brien at Salt River Project shared their useful experience with me. I really appreciate their guidance and support. I also would like to express my gratitude to Dr. George Karady and Dr. Keith Holbert for their time and consideration in being members of my supervisory committee.

TABLE OF CONTENTS

Page

LIST OF TABLES vii

LIST OF FIGURES viii

NOMENCLATURE x

CHAPTER

1 INTRODUCTION 1

1.1 Background 1

1.2 Motivation 2

1.3 Research Goal 2

1.4 Literature Review 3

1.4.1 Literature Review: Cable Components 3

1.4.2 Literature Review: Cable Installations 6

1.4.3 Literature Review: Skin Effect and Proximity Effect 8

1.4.4 Literature Review: Introduction of CYMCAP 9

2 ANALYTICAL APPROACH FOR CABLE THERMAL CALCULATION 11

2.1 Heat Flow Equation 11

2.2 Thermal Resistance 12

2.2.1 Thermal Resistance within the Cable $R_{th1,}$ R_{th2} 12

CHAPTER .....Page

2.2.2 External Thermal Resistance R_{th3} 15

2.2.3 Modification of External Thermal Resistance R_{th3} due to Cyclic Load 19

2.2.4 Modification of External Thermal Resistance R_{th3} due to Backfill 23

2.3 Conductor ac Electrical Resistance R_{ac} 24

2.4 Dielectric Losses W_d 27

2.5 Steady State Rating Equation 30

3 NUMERICAL APPROACH FOR CABLE THERMAL CALCULATION 33

3.1 Input Parameters in CYMCAP 33

3.1.1 Cable Component Parameters 33

3.1.2 Duct Bank Dimension and Material Property Parameters 35

3.1.3 Thermal Backfill Dimension and Material Property Parameters 36

3.1.4 Ambient Temperature and Maximum Conductor Temperature 36

3.1.5 Load curve 36

3.1.6 Heat Sink and Heat Source 37

3.2 Assumptions of SRP 69 kV Cable Systems 37

3.2.1 Ambient Temperature 37

3.2.2 Maximum Conductor Temperature 37

3.2.3 Thermal Resistivity 38

CHAPTER ..... Page

3.2.4 Water Temperature in Arizona Canal 38

3.2.5 Load Factor 38

3.2.6 Cable Depth 42

3.3 CYMCAP Steady State Rating Analysis 42

3.4 CYMCAP Transient Rating Analysis 43

3.4.1 100-Hour Emergency Rating Calculation 43

3.5 Result Summary 46

4 MATHMATICAL MODELS FOR CABLE RATING PREDICTION 51

4.1 Problem Definition 51

4.2 Data Gathering and Preparation 52

4.3 Model Building and Model Evaluation 53

4.3.1 Linear Regression 53

4.3.2 Model Evaluation 54

4.3.3 Nonlinear Regression with Multiple Logarithmic Terms 58

4.3.4 Model Evaluation 60

4.3.5 Nonlinear Regression with Logarithm and Exponential Terms 63

4.3.6 Model Evaluation 64

4.4 Comparison of performance between three methods 67

CHAPTER .....Page

4.5 Conclusion 67

5 SUMMARY AND CONCLUSION 68

REFERENCE..... 70

APPENDIX I 72

APPENDIX II 75

LIST OF TABLES

Table Page

Table 2.1 Cable Construction Parameters 14

Table 2.2 Values for Coefficients k_s and k_p 26

Table 3.1 Thermal Resistivity for Soil and Backfills 38

Table 3.2 Maximum Conductor Temperature in Each Line 44

Table 3.3 Existing Ratings vs Re-evaluated Ratings 48

Table 3.4 Percent Difference Between Existing Ratings and Re-evaluated Ratings 49

Table 3.5 100 and 6 hours Emergency Ratings 50

Table 4.1 Formula Coefficient Calculated by Linear Regression Using 70 Training Data 54

Table 4.2 Regression Equation Transformation 59

Table 4.3 Formula Coefficients Calculated by Linear Regression Using 70 Sampled Data 60

Table 4.4 Formula Coefficient Calculated by Logarithm and Exponential Model Using 70 Sampled Data 64

Table 4.5 Mean Square Error and Maximum Percentage Error between three methods . 67

LIST OF FIGURES

Figure Page

1.1 Cable Bonding Arrangement 5

1.2 Underground Cables in Vertical Arrangement 7

1.3 Underground Cables in Flat Arrangement 7

1.4 Underground Cables in Bored Segment 8

1.5 Illustration of Proximity Effect in Closely Conductors 9

2.1 Single Core Cable Construction 14

2.2 Single Core Cable Construction 17

2.3 Single Core Cable Construction 18

2.4 Grouped of Three Cables and Images 18

2.5 The Daily Load Curve with 75% Load Factor 20

2.6 Illustration of Square I_i and I_{max} Ratio 21

2.7 Cables Installed in Backfill Envelop 24

2.8 Illustration of Dielectric Losses Due to Cable Insulation 28

2.9 The thermal Circuit Representation 30

3.1 Cable Modeling in CYMCAP 35

3.2 Duct Bank Modeling in CYMCAP 36

3.3 Load Factor Calculated for Each Peak 12.5 Days (2006-2012) 40

Figure .....Page

3.4 Papago Buttes-Scottsdale Load Factor Frequency Distribution 40

3.5 Load Factor Calculated for Each Peak 12.5 Days (2006-2012) 41

3.6 Beeline-Pico Load Factor Frequency Distribution 42

3.7 CYMCAP Steady State Simulation 43

3.8 100 Hour Daily Load Curve 45

3.9 Transient Data Table in CYMCAP..... 46

4.1 Illustration of Cable Configuration..... 52

4.2 Linear Model Residual Plot (Training Dataset)..... 55

4.3 Linear Model Residual Plot (Training and Validation Dataset) 56

4.4 Linear Model Residual Duration Curve (Training Data)..... 57

4.5 Linear Model Residual Duration Curve (Training and Validation Data) 57

4.6 Multiple Logarithm Model Residual Plot (Training Dataset)..... 61

4.7 Multiple Logarithm Model Residual Plot (Training and Validation Dataset)..... 61

4.8 Multiple Logarithm Model Error Duration Curve (Training Data) 62

4.9 Multiple Logarithm Model Error Duration Curve (Training and Validation Data) ... 63

4.10 Logarithm and Exponential Model Residual Plot (Training Dataset) 65

4.11 Logarithm and Exponential Model Residual Plot (Training and Validation Dataset)

..... 65

NOMENCLATURE

A	Effective conductor cross section area
b_i	Regression coefficients in linear model
C_d	Capacitance of dielectric insulation
C_0	Capacitance of vacuum medium
c_i	Regression coefficients in logarithm model
d_c	Conductor diameter
d_e	Outer diameter of the cable
d_i	External diameter of insulation
d_x	Fictitious diameter of the cable
e_i	Residual
I_i	Load in i^{th} hour
I_{max}	Maximum load
k_i	Regression coefficients in exponential and logarithm model
k_p	Factor used in calculating y_p
k_s	Factor used in calculating y_s
L	Length of the conductor
$\dot{Q}$	Heat rate through the area A
R_{ac}	ac resistance of the conductor
R_{dc}	dc resistance of the conductor
R_{th1}	Thermal resistivity between conductor and insulation

R_{th2}	Thermal resistivity of jacket
R_{th3}	External thermal resistivity
r_b	Equivalent radius of backfill envelop
r_I	Internal radius of a layer
r_{II}	External radius of a layer
r_1	Radius over conductor
r_2	Radius over insulation
r_3	Radius over sheath
r_4	Radius over outer jacket
S	Sum of the squares of errors
s_1	Horizontal distance between adjacent cables
T	Conductor temperature
u	$2L/d_e$ in 2.2.2
W_c	Joule losses in conductor
W_d	Dielectric losses
W_s	Joule losses in sheath
x_1	Cable size
x_2	Thermal resistivity of duct bank
x_3	Thermal resistivity of native soil
x_4	Cable depth
Y_i	$I_i^2 / I_{\max}^2$ in 2.2.3
y_p	Proximity effect factor

y_s	Skin effect factor
$\hat{y}$	Predicted values
$\hat{y}'$	Transformed value of $\hat{y}$
α_{20}	Temperature coefficient at $20\,°C$
βi	Prediction coefficients
ρ_{soil}	Thermal resistivity of soil
$\tan\delta$	Loss factor of insulation
μ	Loss load factor

1 INTRODUCTION

1.1 Background

Electric energy can be transmitted by overhead power lines or underground cables. Underground distribution is used in populated areas in which overhead lines are not practicable. The main advantages of using underground cables are:

- Esthetically accepted by the public. Overhead lines are not appropriate to build in the proximity of residences due to the esthetics and safety issues.
- Improve power system reliability. The weather issues (wind, ice, snow, and lightning strikes) have less impact on underground lines. External problems caused by vegetation or animals can also be avoided.
- Reduce electromagnetic field (EMF) strength. A magnetic field is induced when electric currents flow through conductors. However, the soil surrounding underground power lines acts as a shielding layer. As a result, the EMF is significantly decreased.
- Cables can be placed underground beneath a street which requires a smaller right-of-way than overhead lines.

However, the main disadvantage of using underground transmission is also obvious. The average duration of the underground line failures are longer than the overhead lines, due to the underground outages are extremely difficult to locate. So it is fairly important to operate the underground lines without exceeding the allowable ratings in a long term cycle.

Ampacity is generally defined as the maximum amount of electric current a device (in our case, a cable) can carry continuously. It is sometimes referred to as the continuous current rating or current carrying capacity of a cable. In the selection of any electrical power cable, ratings, as one of most important factors, must be carefully considered. There are three types of ratings: steady state rating, emergency rating and short circuit cable rating. In this thesis, only steady state and emergency ratings are being studied.

1.2 Motivation

The installations and maintenance of underground cables are far more expensive than overhead lines. For constructing transmission lines of the same distance at the identical voltage level, underground lines cost roughly 4 to 14 times more than overhead lines [1]. The extra cost of underground installation includes the higher cost of the conductors, time to excavate and backfill the cable trenches, and to install the underground cables. The large initial cost associated with cable installations makes it important to carefully select the proper cable types and sizes to serve the loads.

1.3 Research Goal

The goal of this work is to perform thermal studies for Salt River Project (SRP)'s 69 kV underground cable systems using analytical and numerical methods. The analytical approach is to solve the heat transfer problem by creating a thermal circuit. A thermal-electrical analogy has been used to convert complicated heat transfer problems to simple electric circuit problems. The numerical study of SRP's 69 kV underground lines involves steady state ratings calculation, conductor temperature calculation based on peak

loadings with the aid of computational software CYMCAP. Finally, a nonlinear regression method using simulated data has been developed to estimate the SRP's underground cables steady state ratings.

1.4 Literature Review

1.4.1 Literature Review: Cable Components

Power cable components consist of conductor, conductor insulation, sheath and jacket. The electrical insulation layer separates the electrical conductor from other cable components through which the current might flow. Sheath (or concentric neutral wires) acts as a layer placed over insulation surface to provide a path for the induced current flowing to the ground. For the majority cables, the jacket is necessary as a covered to prevent external corrosion, degradation due to sunlight, environmental water, or physical abuse. The following is a list of cable aspects that are relevant to this research.

- Conductor

There are two materials usually used in cable conductors: copper and aluminum. In this thesis, the underground cables are all copper wires. The cross section of conductor can be either solid or stranded. Stranded conductors comprise a group of wires which can be either segmented or compacted to provide more flexibility than solid cable.

Conductor sizes are described in thousand circular mils (MCM) or kilo circular mils (*kcmil*). A circular mil (*cmil*) is defined as the area of a circle with a diameter of one mil (0.001 inch). Typical 69 kV conductor sizes are 1000 *kcmil* through 2750 *kcmil*. Cables with larger conductor cross section areas have lower electric resistance losses and

are able to dissipate the heat better than those with smaller cables. As the wire gauge becomes smaller, the wire becomes larger in diameter. So No. 10 AWG is larger cross section than No. 14 AWG.

- Conductor shield

The conductor shield is a layer between conductor and insulation which is usually made of a semi-conductor material. The primary benefit of the shield (or screen) is to achieve a radially symmetric electric field and smooth out the conductor contour as well.

- Insulation

The conductors are typically insulated with oil-impregnated paper or extruded solid dielectrics which are most widely used presently. Many types of solid extruded insulations are currently in use: natural rubber, butyl rubber, high molecular weight polyethylene (HMWPE), Polyethylene (PE), and Crosslinked polyethylene (XLPE). There is a strong relationship between insulation type and cable ratings [2]. It becomes desirable to select insulation material with low thermal resistivity to reach a favorable heat dissipation condition. Taking advantage of low dielectric losses, XLPE has been dominantly used as insulation in medium or high voltage power cables today.

- Insulation shield

The underground cables can be seen as a cylindrical capacitor with an insulation shield that operates as the external conducting plate and with insulation that acts as the dielectric medium. There are three purposes for insulation shield: (1) provide symmetric

electrical field distribution within the insulation, (2) relief of the surge voltage by making uniform capacitance to equalize surge impedance along the cable, (3) the metallic portion provides a low impedance path for charging current to flow to ground. Therefore, the insulation shield should be carefully considered in cable design.

- Sheaths / concentric neutral wires

The sheath is a protection covering over insulation. The main function of the sheath is to improve mechanical strength and protect cables against moisture, chemical corrosion and physical abuse. The sheaths are either nonmetallic (natural rubber, PVC) or metallic material (lead, aluminum). Metallic sheaths provide the return path for fault currents. Sometimes instead of sheaths, fault currents are carried by concentric neutral wires. Since the induced current will flow on the surface of the metallic sheaths, they must be connected to the ground at least at one point. Two common sheaths /concentric-neutral-wires-bonding methods are typically used for three-phase power distribution: single point bonding and crossbonding.

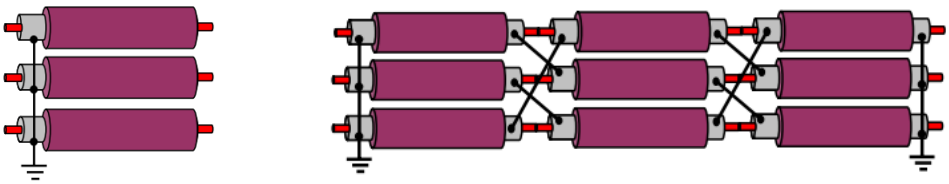

(a) single-point bonding (b) crossbonding

Fig. 1.1 Cable Bonding Arrangement

Fig. 1.1 (a) shows the single-point bonding in which the sheaths are grounded at one place. Since there is no closed path for circulating currents, sheath losses would be

avoided as a result. However, a high potential point will occur at the further end along the cable. The crossbonding technique is shown in Fig. 1.1 (b). The purpose of crossbonding is to reduce or even eliminate circulating currents by dividing the sheath into three equal segments. If the lengths of each segment are equal, then the circulating currents have the same phase separation and cancelled each other.

- Jackets

Various nonmetallic materials could be used as jackets of cables such as Polyethylene (PE), Ethylene Propylene Rubber (EPR), and PVC. The jacket is the most exterior layer that protects the underlying conductor against cable failures caused by either external electrical or mechanical damage.

1.4.2 Literature Review: Cable Installations

The cable ampacity calculations are performed based on the cable burial conditions. In urban areas, cables are always enclosed in PVC conduits and one or multiple circuits are laid in a concrete duct bank. There are three typical types of cable arrangements. The most common cable laying method is to put two three-phase circuits vertically in a concrete duct bank. There are also two spare conduits available at the top of the duct bank for future use. Such arrangement is shown in Fig. 1.2. When the installation has a duct bank height limitation, two paralleled circuits are in flat arrangement (Fig. 1.3).

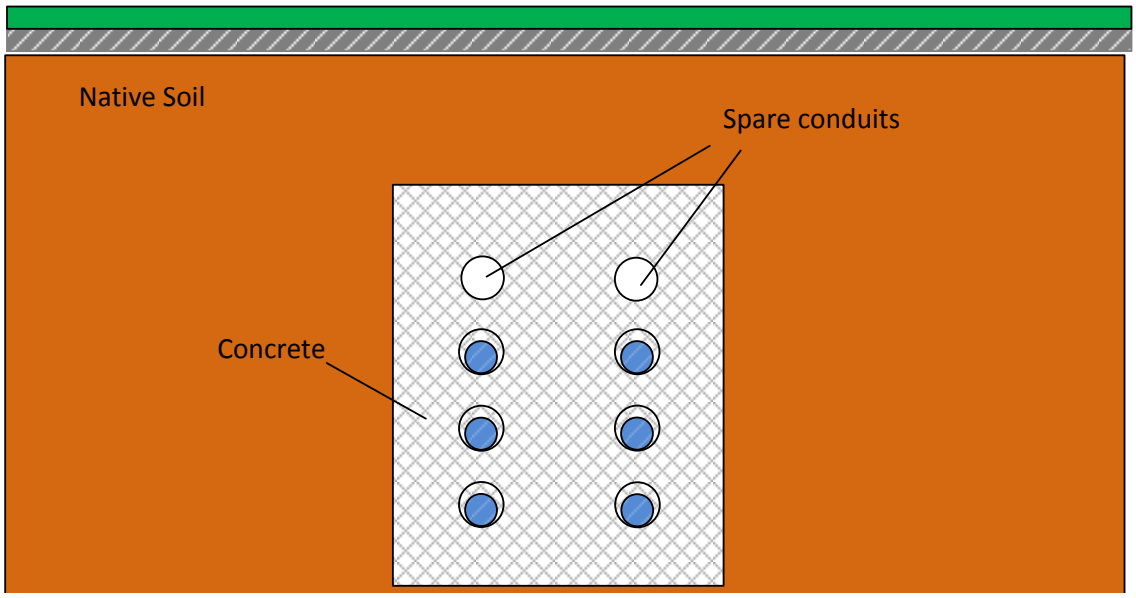

Fig. 1.2 Underground Cables in Vertical Arrangement

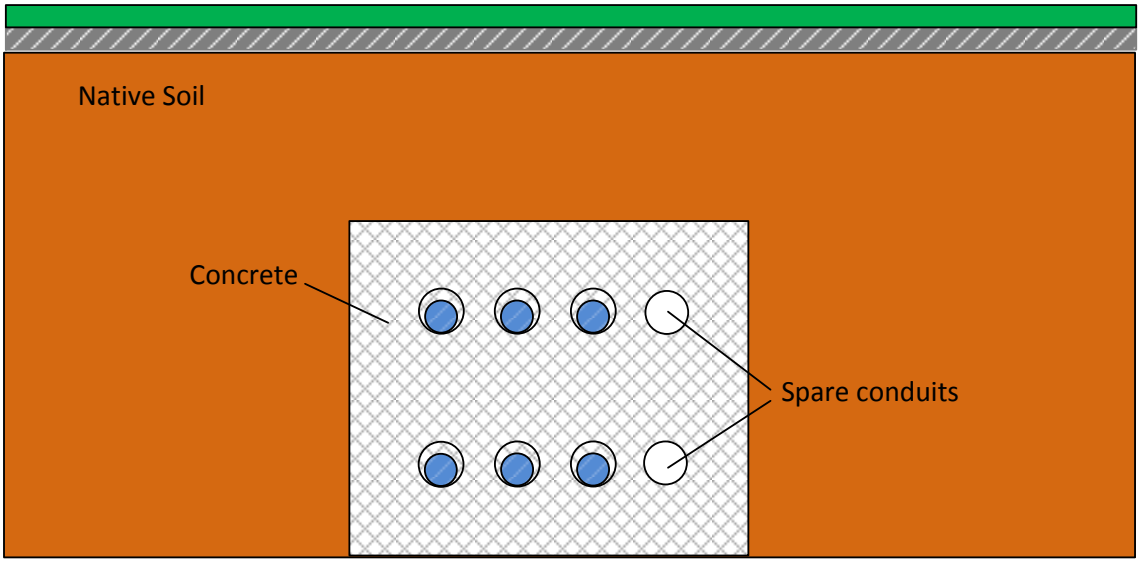

Fig. 1.3 Underground Cables in Flat Arrangement

In urban areas, there is often a need to put underground cables underneath rivers, railway tracks or other obstacles. In such cases, a drilling method called horizontal directional boring is often applied. The advantage of using directional boring is to install

underground power cables without trenching. Fig. 1.4 shows a typical cross section of power cables in a bored pipe.

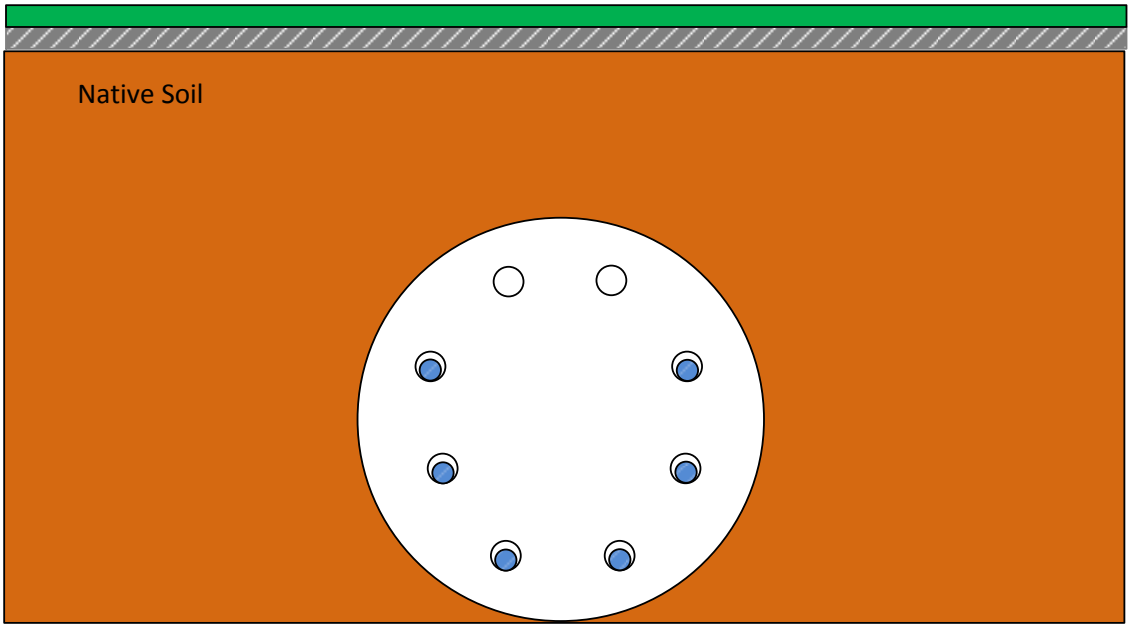

Fig. 1.4 Underground Cables in Bored Segment

1.4.3 Literature Review: Skin Effect and Proximity Effect

Skin effect is name applied to phenomenon in alternative current circuits where the current tends to flow on the surface of the conductor causing that the current density at the surface to be greater than at the center of the conductor. Due to skin effect, the effective cross section of conductor when carrying an ac current is effectively decreased and the ac resistance is higher than dc resistance as a result.

Proximity effect also increases the effective resistance when conductor is carrying ac current. Proximity effect is a phenomenon that occurs when two conductors carry ac current in the same direction and close to each other. Under this scenario, the current density on the remote sides is larger than conductor sides adjacent to each other shown as

the upper two conductors in Fig. 1.5. On the other hand, two bottom conductors in Fig. 1.5 with opposite current direction will result in high current density on the cable sides that are in close proximity.

Fig. 1.5 Illustration of Proximity Effect in Closely Conductors

1.4.4 Literature Review: Introduction of CYMCAP

CYMCAP (CYME Cable Ampacity Calculations) is a power engineer tool package developed by CYME International. CYMCAP is a computer aided electrical software designed to perform ampacity ratings calculation and cables temperature calculations. CYMCAP is an easy-to-use commercial software application that offers steady-state and transient cable thermal calculations. These calculations are fully consistent to North American practice and IEC 287 and IEC 853 International standards.

CYMCAP analytical capabilities:

- Provide databases for typical cables, ductbanks and load curves
- User-defined cable constructions
- User-defined ductbanks. Users can customize the dimensions and thermal resistivity of the duct banks.
- User-defined load curves. Users can customize the load curve for each circuit.

- Visualized cable configurations. This feature allows users to specify the distance between different conductors/circuits.
- Various cable installation conditions. These include directly buried cables, thermal backfill, and duct banks.
- Modeling of heat sources and heat sinks provided by nearby cables.

2 ANALYTICAL APPROACH FOR CABLE THERMAL CALCULATION

The analytical approach used in this thesis is solely to compute steady state ampacity of flat arrangement cables contained within thermal backfill. This approach is applied to a scenario in which three 2000 *kcmil* cables are installed in a duct bank. Detailed cable installation configuration is shown in Fig. 2.7. The thermal resistivity of insulation, thermal resistivity of outer jacket and thermal resistivity of soil are assumed constant.

2.1 Heat Flow Equation

The cable ampacity is defined as the maximum current continuously carried by a conductor within temperature rating [3]. Electric current flowing through the conductor of a cable results in temperature rises: heat is transferred from the conductor to the ambient environment through insulation. The temperature rating is a function of the thermal degradation the insulation can withstand without deterioration that can lead to a fault under transient over-voltages. Before introducing the ampacity calculations, a review of the heat transfer mechanism is introduced first.

Heat transfer is always from warmer object to colder objects by three basic mechanisms: conduction, convection and radiation. For underground cables, heat is transferred by conduction from conductor to outer layers and ambient environment. The equation for heat conduction is derived from Fourier's law

$$\dot{Q} = -\frac{A}{\rho}\frac{dT}{dx} \tag{2.1}$$

where $\dot{Q}$ (W) is the heat energy (rate) transferred through a given surface, ρ (K · m/W) is the thermal resistivity of heat conducting material, *T* is the conductor temperature and *A* is effective conductor area. This expression indicates that heat rate, $\dot{Q}$, is proportional to the temperature gradient d*T*/d*x* and the minus sign means that heat flows in the direction of decreasing temperature.

2.2 Thermal Resistance

The cable ratings calculation is based on the parameters in the thermal circuit (described in 2.5) whose values depend, among several things, on soil resistivity and heat transfer coefficients [4]. Therefore, the higher the accuracy of the thermal circuit parameters the smaller the error in the cable carrying capability calculated.

2.2.1 Thermal Resistance within the Cable R_{th1}, R_{th2}

Heat is generated from the conducting material within the power cable and the dielectric (non-conducting) material impedes heat transfer. Thus thermal resistance indicates the material's resistance to heat flow.

Equation (2.1) defines the heat rate at a given surface. This equation may be modified to become applicable in a cable heat transfer model. In other words, the equation in cylindrical coordinate becomes

$$\dot{Q} = -\frac{2\pi r L}{\rho}\frac{dT}{dr} \tag{2.2}$$

where *r* (m) is the dependent variable in cylindrical coordinate system, *L* (m) is the length of cable. Assuming that the inner layer surface temperature is T_1 and outer surface

temperature is T_2 and the internal and external radius of this layer is r_{I} and r_{II}, respectively. Equation (2.2) may be integrated as follows:

$$\frac{\dot{Q}}{\frac{2\pi L}{\rho}} \ln \frac{r_{II}}{r_I} = T_I - T_{II} \tag{2.3}$$

The heat flow can be described by analogy to electrical circuit which electrical engineers are familiar with. Consequently, an analogy between electrical resistance and thermal resistance can be achieved. As resistance is the ratio of potential difference to the current through it, the thermal resistance R_{th} ($\mathrm{K} \cdot \mathrm{m/W}$) per unit length of a cylindrical conductor is

$$R_{th} = \frac{\rho}{2\pi} \ln \frac{r_2}{r_1} \tag{2.4}$$

Therefore, the thermal resistance between one conductor and insulation the shield R_{th1} ($\mathrm{K} \cdot \mathrm{m/W}$), and the thermal resistance of jacket R_{th2} ($\mathrm{K} \cdot \mathrm{m/W}$) can be computed, respectively from Equation (2.4).

$$R_{th1} = \frac{\rho_{th1}}{2\pi} \ln \frac{r_2}{r_1} \tag{2.5}$$

$$R_{th2} = \frac{\rho_{th2}}{2\pi} \ln \frac{r_4}{r_3} \tag{2.6}$$

where r_1 is radius of a circle circumscribing a conductor, r_2 is radius over insulation, r_3 is radius of a circle of circumscribing sheath, and r_4 is radius over outer jacket. These parameters are illustrated in Figure 2.1. The variables ρ_{T_1} and ρ_{T_2} ($\mathrm{K} \cdot \mathrm{m/W}$) are thermal resistivities of the insulation and jacket, respectively.

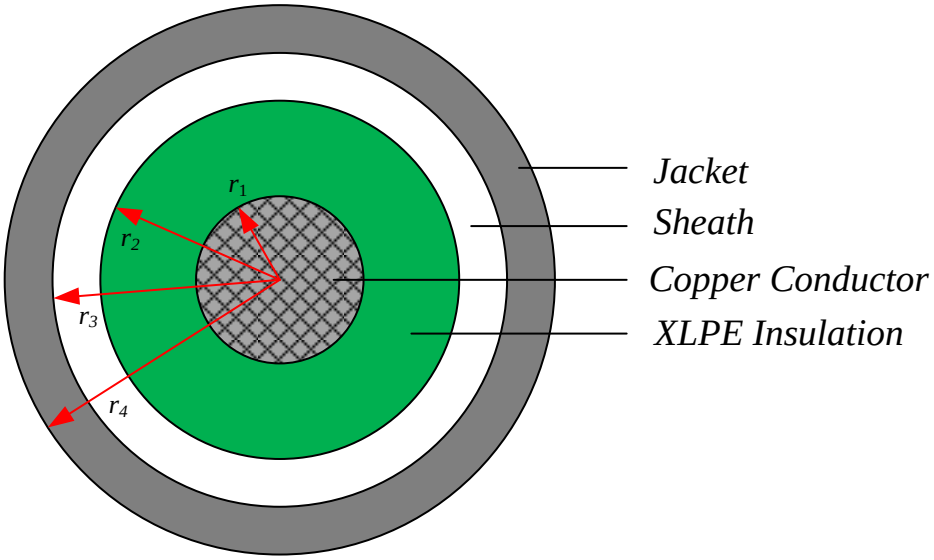

Fig. 2.1 Single Core Cable Construction

Example 2-1: Fig. 2.1shows a single core cable with 2000 *kcmil* copper conductor that has the parameters listed in Table 2.1.

Table 2.1 Cable Construction Parameters

Cable construction	Outer diameter (inch)
Conductor copper 2000*kcmil*	1.58
Semiconducting screen	1.68
450 mils XLPE insulation	2.58
Insulation screen	2.79
42 AWG 14 copper concentric wires	2.92
Insulation jacket	3.29

Thermal resistance between conductor and insulation shield R_{th1} is obtained by Equation (2.5), and thermal resistance of jacket R_{th2} is determined by Equation (2.6). Therefore, R_{th1}=0.3196 K · m/W, R_{th2}=0.0665 K · m/W.

2.2.2 External Thermal Resistance R_{th3}

The surrounding environment of the underground cables (soil/backfill), which acts as the external thermal resistance, has a great effect on cable ampacity ratings. Numerous early works were done in external thermal resistance calculation. Using the thermal-electrical analogous circuit, the underground cables were usually modeled as paralleled conducting cylinders with equal charges by early researchers. Poritsky developed a formula to determine the potential distribution of two infinitely long conducting cylinders with equal radii [5]. Goldenberg derived equations for calculating external thermal resistance with the assumption that superposition is applicable [6].

The analytical approach presented in this thesis assumes that (i) superposition is applicable (ii) the earth surface is isothermal (iii) the center conductor is the hottest. Since superposition is applied to calculate the external thermal resistance of grouped cables which might be difficult to deal with, it is easier to start from determining the thermal resistance of an isolated single buried cable. External thermal resistance for single buried cable is obtained from [6]

$$R_{th3} = \frac{\rho_{soil}}{2\pi} \ln(u + \sqrt{u^2 - 1}) \qquad (2.7)$$

where

$$u = \frac{2L}{d_e} \tag{2.8}$$

L (m) is the distance from the surface of the ground to cable axis, d_e (m) is the outer diameter of the cable, and ρ_{soil} (K·m/W) is the thermal resistivity of soil. When u is more than 10, Equation (2.7) can be reduced to (2.9) with a significant loss in accuracy.

$$R_{th3} = \frac{\rho_{soil}}{2\pi} \ln(2u) \tag{2.9}$$

For grouped cables, the image method has been applied to model the mutual cable heating [9]. Then the formula used to calculate grouped cables R_{th3} can be obtained by modifying Equation (2.7). The R_{th3} of the p_{th} cable is given by,

$$R_{th3} = \frac{\rho_{soil}}{2\pi} \ln\left((u + \sqrt{u^2 - 1}) \left((\frac{d'_{p1}}{d_{p1}})(\frac{d'_{p2}}{d_{p2}})...(\frac{d'_{pk}}{d_{pk}})...(\frac{d'_{pq}}{d_{pd}}) \right) \right) \tag{2.10}$$

where d_{p1},d'_{p1} are the distance from the p^{th} conductor to 1^{th} conductor and its image, respectively, as illustrated in Fig. 2.3. The equation is valid provided the cables are equally loaded. This equation, (2.10), has taken the mutual heating into account. If we assume the cable configuration is flat arrangement as shown in Figure 2.2, then we get

$$d_{p1} = d_{p2} = s_1 \tag{2.11}$$

$$d'_{p1} = d'_{p2} = \sqrt{s_1^2 + (2L)^2} \tag{2.12}$$

where s_1 is the horizontal distance between cables shown in Fig. 2.4.

After determining $d_{p1}, d_{p2}, d'_{p1}, d'_{p2}$, these values may be substituted into (2.10). The external thermal resistance of the cables then becomes:

$$R_{th3} = \frac{\rho_{soil}}{2\pi} \ln\left((u + \sqrt{u^2 - 1}) \left(\left(\frac{\sqrt{s_1^2 + (2L)^2}}{s_1} \right) \left(\frac{\sqrt{s_1^2 + (2L)^2}}{s_1} \right) \right) \right) \qquad (2.13)$$

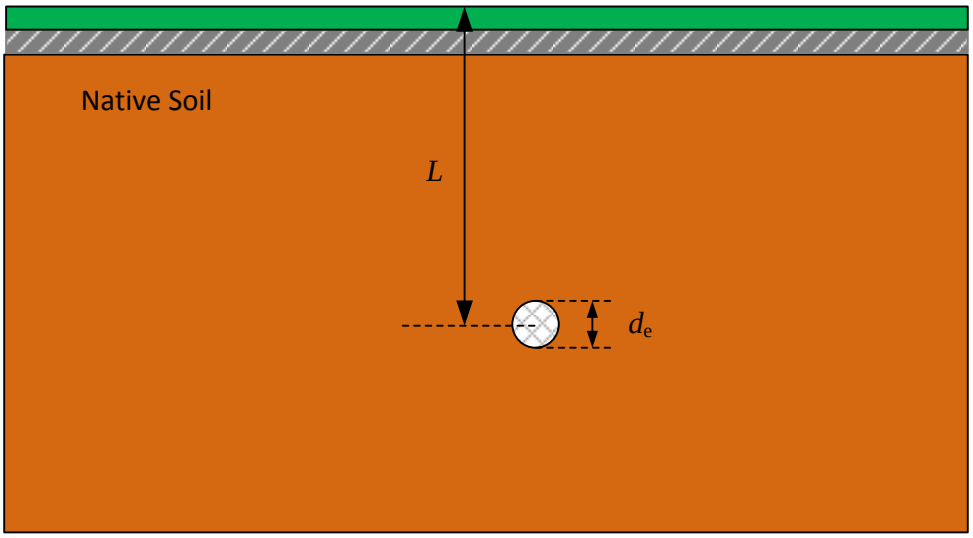

Fig. 2.2 Single Core Cable Construction

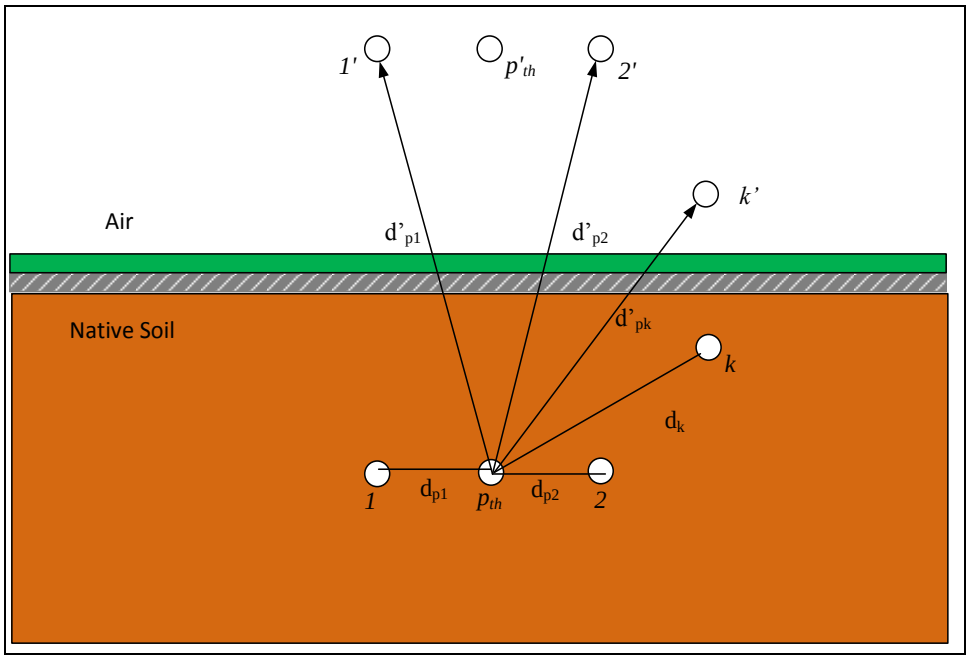

Fig. 2.3 Single Core Cable Construction

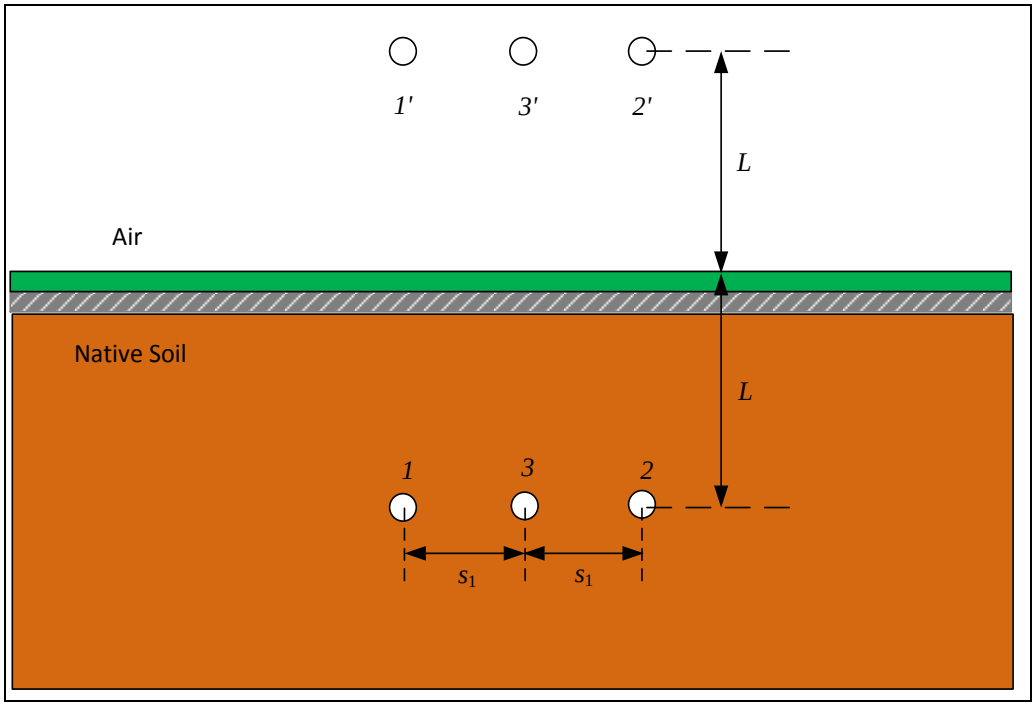

Fig. 2.4 Grouped of Three Cables and Images

2.2.3 Modification of External Thermal Resistance R_{th3} due to Cyclic Load

Since the steady state ampacity rating in this thesis is the cyclically loaded cable rating (described in section 1.1), it is necessary to use a computational method implemented with a load factor to perform the cyclic ratings calculation. Goldenberg developed an approach to incorporate load factor by changing the value of external thermal resistance R_{th3}. This method starts from calculating the loss factor, μ. In 1956, Goldenberg took the load factor into account in the thermal resistance calculation by using the loss load factor μ. The loss load factor is defined as the ratio of average load loss and the peak load loss. The single day loss factor is calculated by decomposing daily load cycle into one-hour rectangular pulses. The total number of rectangular pulses during a day is 24. Loss factor μ is given by,

$$\mu = \frac{1}{24} \frac{\sum_{i=0}^{23} I_i^2}{I_{max}^2} \tag{2.12}$$

The loss factor is explained through the example 2-1. A daily load curve is shown in Fig. 2.5 The Daily Load Curve with 75% Load Factor.

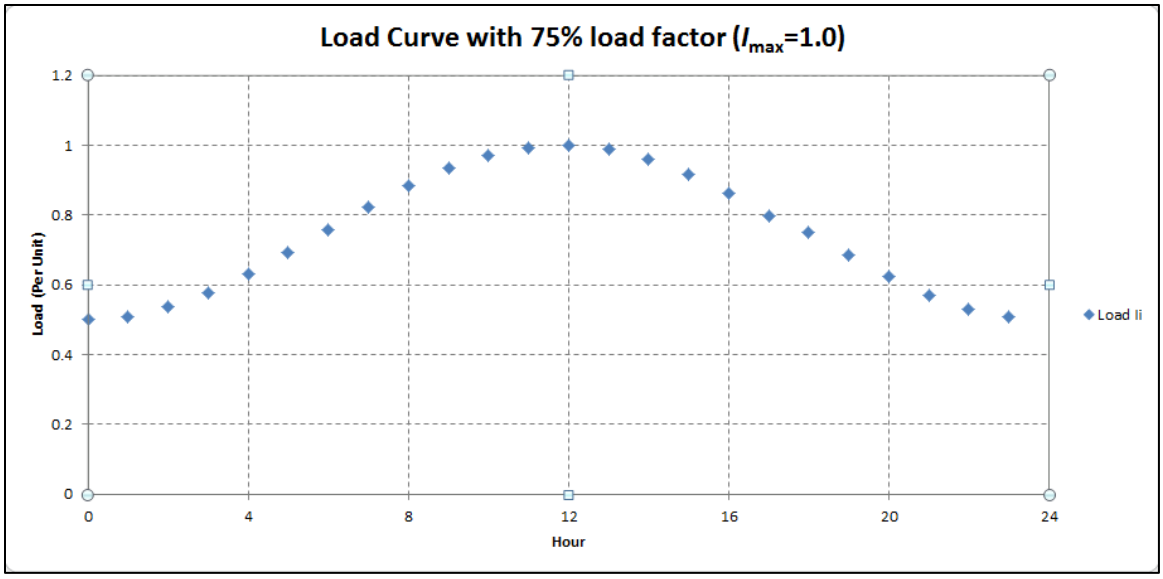

Fig. 2.5 The Daily Load Curve with 75% Load Factor

To simplify the Equation (2,12), Y_i has been introduced.

$$Y_i = \frac{I_i^2}{I_{\max}^2} \tag{2.13}$$

Then the (2.12) becomes,

$$\mu = \frac{1}{24}\sum_{i=0}^{23} Y_i \tag{2.14}$$

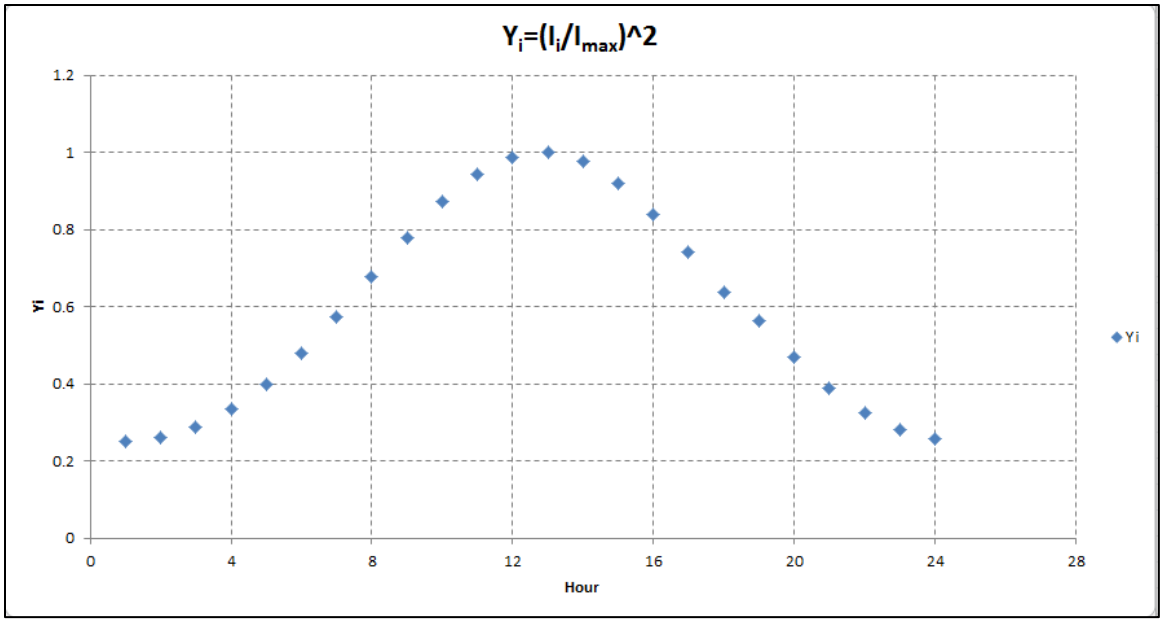

Fig. 2.6 Illustration of Square I_i and I_{max} Ratio

In example 2-1, the loss factor is,

$$\mu = \frac{0.2500 + 0.2599 + 0.2876 + .. + 0.2577}{24} = 0.5938$$

Neher (1953) proposed that the heat flow during a cyclic load can be decomposed into two components, steady state component and transient component. The transient component $R_{th3,tran}$ will only result in heat flow to a limited distance from the cable. Assume the thermal resistance of the transient component $R_{th3,tran}$ will be smaller than its counterpart steady state component $R_{th3,ss}$. The external thermal resistance R_{th3} can be modified as follows [7]:

$$R_{th3} = \mu R_{th3,ss} + (1-\mu) R_{th3,tran} \qquad (2.15)$$

The transient component can be represented by [7],

$$R_{th3,tran} = \frac{\rho_{soil}}{2\pi} \ln \frac{d_x}{d_e} \tag{2.16}$$

where d_e (m) is the outer diameter of the cable. The fictitious diameter d_x for sinusoidal load variation is given by Heinhold [8]:

$$d_x = \frac{205}{\sqrt{w}\rho_{soil}^{0.4}} \tag{2.17}$$

where w is the number of load cycles in a 24 hour period.

The external thermal resistance in Equation (2.15) can be written as

$$R_{th3} = \frac{\rho_{soil}}{2\pi} \left[\mu \ln \frac{4L}{d_e} + (1-\mu) \ln \frac{d_x}{d_e} \right] \tag{2.18}$$

$$R_{th3} = \frac{\rho_{soil}}{2\pi} \left[\ln \frac{d_x}{d_e} + \mu \ln \frac{4L}{d_x} \right] \tag{2.19}$$

If taking a group of cables into consideration, (2.10) is generated through multiplying the term $u + \sqrt{u^2 - 1}$ in (2.7) by $(\frac{d'_{p1}}{d_{p1}})(\frac{d'_{p2}}{d_{p2}})...(\frac{d'_{pk}}{d_{pk}})...(\frac{d'_{pq}}{d_{pd}})$. Equation (2.19) can be reformulated for equally loaded cables by doing the same thing as in (2.10)

$$R_{th3} = \frac{\rho_{soil}}{2\pi} \left\{ \left\{ \ln \frac{d_x}{d_e} + \mu \ln \left[\frac{4L}{d_x} \right] \cdot \left[\frac{d'_{p1}}{d_{p1}} \frac{d'_{p2}}{d_{p2}} \frac{d'_{p3}}{d_{p3}} ... \frac{d'_{pk}}{d_{pk}} \right] \right\} \right. \tag{2.20}$$

The external thermal resistance in example 2-1 can be calculated as follows. The parameters for example 2-1 are L=4 ft,d_{p1}=d_{p2}=1 ft, d'_{p1}=d'_{p2}=$\sqrt{L^2+1}$ =8.062 ft, ρ_{soil}=1.20K·m/W, d_e=3.29 in, the fictitious diameter d_x is computed by (2.17) and equals

7.503 in. u=4L/d_x=25.58. Therefore, the external thermal resistance R_{th3} with loss factor μ=0.5938 calculated by (2.20) is 1.0771K·m/W.

2.2.4 Modification of External Thermal Resistance R_{th3} due to Backfill

If the underground cables are directly installed in the trench with native soil as the backfill, the heat generated by cable conductors is hard to dissipate due to the poor thermal property of the native soil. Underground systems at the sub-transmission level, such as SRP's 69 kV underground cables, are to be installed in a thermally hospitable environment. This can be achieved by using fluidized thermal backfill (FTB) as backfill which consists of sand, cement and fly ash.

Since the fluidized thermal backfill has a lower thermal resistivity, the effect of backfill thermal resistivity can be taken into account by adding a correction term in external thermal resistance.

$$R_{th3,corr} = \frac{n}{2\pi}\left(\rho_{soil} - \rho_{bf}\right)\ln\left(u + \sqrt{u^2 - 1}\right) \tag{2.21}$$

where n is the number of cables placed in backfill envelop. ρ_{bf} is the thermal resistivity of backfill. The variable r_b is the equivalent radius of backfill envelop and $u=L/r_b$. The calculation of r_b is associated with the height and width of the backfill envelop [9].

$$r_b = \exp\left[\frac{x}{2y}\left(\frac{4}{\pi} - \frac{x}{y}\right)\ln\left(1 + \frac{y^2}{x^2}\right) + \ln\frac{x}{2}\right] \tag{2.22}$$

The correction term for the external thermal resistance of example 2-1 can be calculated as follows. First using (2.22) with x=3 ft, y=4 ft, the equivalent radius of

envelop r_b is calculated as 1.833 ft. $u=L/r_b=2.182$. The backfill thermal resistivity is 0.95 K·m/W. Therefore, after taking the backfill into account, the correction term is given by,

$$R_{th3,corr} = \frac{3}{2\pi}(1.20-0.95)\ln\left(u+\sqrt{u^2-1}\right)=0.169K\cdot m/W$$

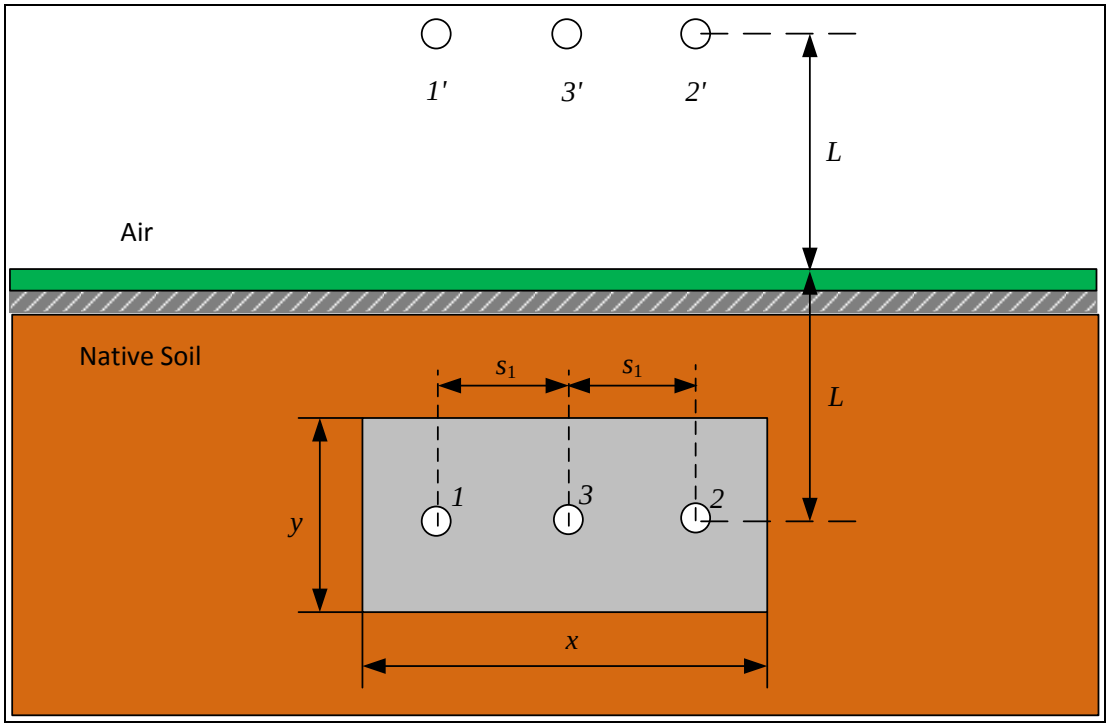

Fig. 2.7 Cables Installed in Backfill Envelop

The external thermal resistance will be the summation of Equation (2.20) and (2.21). R_{th3}=1.0771+0.1690=1.2461K·m/W.

2.3 Conductor ac Electrical Resistance R_{ac}

The cable heat losses can be expressed by introducing alternating current (ac) resistance in the following equation

$$W_c = I^2 R_{ac} \qquad (2.23)$$

where W_c (W/m) is the heat losses or Joule losses of the conductor, R_{ac} (ohm/m) is the ac resistance of the conductor. In order to perform cable rating calculations, it is necessary to compute ac resistance first.

When the conductor temperature is $20\,°C$, the dc resistance per unit length R_{20} (ohm/m) is expressed as,

$$R_{20} = \frac{\rho_{20}}{A} \tag{2.24}$$

where ρ_{20} (ohm·m) is electrical resistivity of conductor. For copper, $\rho_{20} = 1.7241 \times 10^{-8}$

Because the conductor resistance changes with temperature, the actual dc resistance R_{dc} (ohm/m) at temperature T is obtained as

$$R_{dc} = R_{20}(1 + \alpha_{20}(T - 20)) \tag{2.25}$$

where α_{20} is temperature coefficient at $20\,°C$. For copper conductor, $\alpha_{20} = 3.93 \times 10^{-3}$ and T is corresponding conductor temperature. The relationship between ac resistance and dc resistance can be expressed as,

$$R_{ac} = R_{dc}(1 + y_s + y_p) \tag{2.26}$$

where R_{dc} (ohm/m) is dc resistance, y_s is skin effect factor and y_p is proximity effect factor. The ac resistance is always higher than dc resistance due to the imbalanced distribution of current that are caused by the skin effect and proximity effect, which are described in section 1.6. The skin effect factor y_s is written as [10],

$$y_s = \frac{x_s^4}{192 + 0.8x_s^4} \tag{2.27}$$

where

$$x_s^2 = \frac{8\pi f}{R_{dc}} 10^{-7} k_s \tag{2.28}$$

where f (Hz) is electrical frequency, and the k_s values for different cable configurations are given in Table 2.2 [10].

Table 2.2 Values for Coefficients k_s and k_p

Type of conductor	Whether dried and impregnated or not	k_s	k_p
Round, stranded	Yes	1	0.8
Round, stranded	No	1	1
Round, compact	Yes	1	0.8
Round, compact	No	1	1
Round, 4 segments	Either	0.435	0.37
Sector-shaped	Yes	1	0.8
Sector-shaped	No	1	1

The proximity effect factor y_p is given by [10],

$$y_p = \frac{x_p^4}{192 + 0.8x_p^4} \left(\frac{d_c}{s}\right)^2 \left[0.312\left(\frac{d_c}{s}\right)^2 + \frac{1.18}{\frac{x_p^4}{192 + 0.8x_p^4} + 0.27} \right] \tag{2.29}$$

where,

$$x_p^2 = \frac{8\pi f}{R_{dc}} 10^{-7} k_p \tag{2.30}$$

dc (m) is the conductor diameter, *s* (m) is the distance between conductor axes, and k_p is given in Table 2.2. The R_{ac} can be obtained by putting y_s and y_p into Equation (2.8).

For example 2-1, dc resistance R_{dc} (ohm/m) at 90 ^{0}C is given by Equation (2.25)

$$R_{dc} = R_{20}(1+\alpha_{20}(T-20)) = 1.7241\times10^{-8}\left(1+3.93\times10^{-3}(90-20)\right) = 2.224\times10^{-5}\Omega/m$$

Compute x_s by Equation (2.28) with R_{dc} and k_s=1, then x_s equals to 2.6039. Compute x_p by Equation (2.30) with k_p=1, then x_p equals to 0.2009. The skin effect factor y_s and proximity effect factor y_p are obtained by Equation (2.9) and (2.11), respectively.

$$y_s = \frac{x_s^4}{192+0.8x_s^4} = \frac{2.6039^4}{192+0.8\times2.6039^4} = 0.2010$$

$$y_p = \frac{x_p^4}{192+0.8x_p^4}\left(\frac{1.58}{12}\right)^2\left[0.312\left(\frac{1.58}{12}\right)^2 + \frac{1.18}{\frac{x_p^4}{192+0.8x_p^4}+0.27}\right] = 0.0087$$

From Equation (2.26), the ac resistance is achieved R_{ac}=2.6904·10^{-5} Ω/m

2.4 Dielectric Losses W_d

All dielectrics create losses are of two types: conducting losses, polarization losses. The conducting losses are caused by the ability to pass the charge through a dielectric. On the other hand, polarization losses represent the ability to store the charge. The dielectric losses are the comprehensive losses of conducting losses and polarization losses. In the

electrical analog circuit to the thermal problem, the cable insulation resulting in dielectric losses can be modeled by a resistor and capacitor connected in parallel as shown in Fig. 2.8. The current through insulating dielectric, I_d, consist of two parts: the capacitive current, I_c , and resistive current I_r.

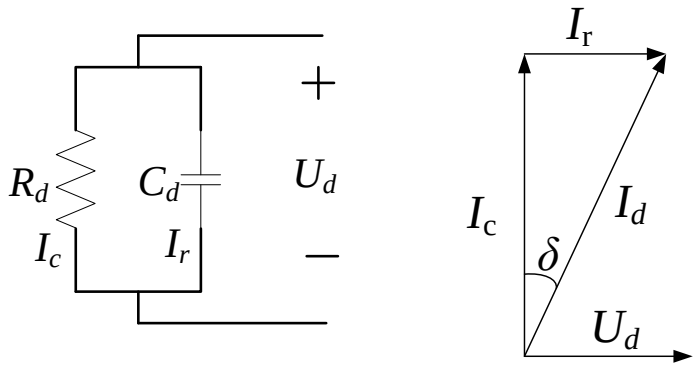

(a) equivalent circuit for insulation (b) U-I relationship

Fig. 2.8 Illustration of Dielectric Losses Due to Cable Insulation

The capacitance of the dielectric insulation C_d (F/m) is given by

$$C_d = \varepsilon \cdot C_0 \tag{2.31}$$

where

$$C_0 = \frac{10^{-9}}{18 \ln(\frac{d_i}{d_c})} \tag{2.32}$$

The variable C_0 (F/m) is the capacitance with vacuum as medium. Dielectric constant ε is the relative permittivity of the capacitance when the frequency is zero. Variable d_i is the external diameter of insulation excluding screen, d_c is the conductor diameter including

screen. After obtaining the equivalent capacitance of the insulation C_d, the dielectric loss per unit length is given by [10],

$$W_d = \frac{U_d^2}{R_d} = \omega C_d U_d^2 \tan\delta \tag{2.33}$$

where

$$\tan\delta = \frac{I_r}{I_c} = \frac{U_d / R_d}{U_d \omega C_d} = \frac{1}{R_d \omega C_d} \tag{2.34}$$

Variable tanδ is called the dielectric loss factor, and the δ is the angle between resistive current and capacitive current (see Fig. 2.8 (b)). In the cable rating calculation, values of tanδ for typical materials are given in Table 2.3.

Table 2.3 Values for coefficients ε and tanδ

Cable type	ε	tanδ
Cable insulated with impregnated paper	4	0.01
Fluid-filled low-pressure (up to 87kV)	3.6	0.0033
Fluid-filled, pipe type	3.7	0.0045
Butyl rubber	4	0.05
PVC	8	0.1
PE (HD and LD)	2.3	0.001
XLPE above18/30 (36)kV unfilled	2.5	0.001
XLPE above18/30 (36)kV filled	3	0.005

Therefore, in example 2-1, dielectric losses W_d is 1.017 W/m using Equation (3.33).

2.5 Steady State Rating Equation

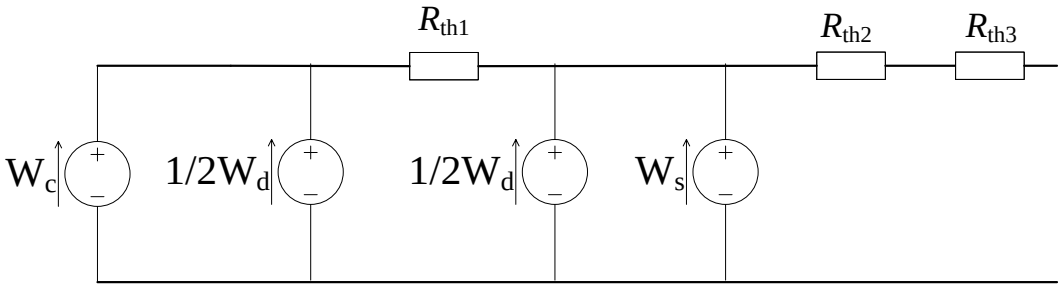

Fig. 2.9 The thermal Circuit Representation

All the parameters discussed in sections 2.1.2, 2.1.3 and 2.1.4 will be used in cable steady state rating calculation. As shown in Fig. 2.9, the cable thermal circuit is constructed to derive the ampacity equation. The thermal-electrical analogy is therefore applied to simplify the problem. Since heat is analogous to current flow in the analog

electrical circuit, the heat losses, W_c, W_d, W_s, are equivalent to current sources. Similarly, the temperature at different points is analogous to potential at each node. Then the temperature difference between conductor and ambient can be expressed by

$$\Delta T = \left(W_c + \frac{1}{2} W_d \right) R_{th1} + \left(W_c + W_d + W_s \right) \left(R_{th2} + R_{th3} \right) \tag{2.35}$$

where conductor losses W_c and dielectric losses W_d are given by equations in section 2.3, section 2.4, respectively. Thermal resistance of insulation R_{th1}, thermal resistance of outer jacket R_{th2} and external thermal resistance R_{th3} are discussed in section 2.1.2.

Joule losses in sheath W_s can be written as [10]

$$W_s = \lambda_1 \cdot W_c \tag{2.36}$$

where λ_1 is the sheath loss factor and defined as the ratio of cable sheath losses to conductor losses.

To solve for the steady state rating of underground cable, electric current flowing on the cable must be introduced into Equation 2.17. Since the conductor loss is given by equation 2.7, it is convenient to replace W_c by $I^2 R_{ac}$ in Equation (2.35). Finally, the steady state rating can be calculated as following

$$I = \sqrt{\frac{\Delta T - \left(\frac{1}{2} R_{th1} + R_{th2} + R_{th3} \right) W_d}{R_{ac} R_{th1} + R_{ac} \left(1 + \lambda_1 \right) \left(R_{th2} + R_{th3} \right)}} \tag{2.37}$$

In example 2-1, the steady state rating is obtained by using above Equation (2.37) by inserting the following pararmeters. The maximum conductor temperature is taken as

90 ^{0}C, which was described in section 3.2.2. ΔT=90 ^{0}C-35 ^{0}C=55 ^{0}C, R_{th1}=0.3196K·m/W, R_{th2}=0.0665K·m/W, R_{th3}=1.2461K·m/W, W_d=1.017 W/m, R_{ac}=2.6904·10^{-5} Ω/m, λ_1=0. The steady state rating is 1103.8A

3 NUMERICAL APPROACH FOR CABLE THERMAL CALCULATION

Numerical calculation have been performed to develop the steady state and transient cable ratings for SRP's 69 kV underground cable installations by using the commercial software CYMCAP. CYMCAP is especially designed to perform cable ampacity and conductor temperature calculations under various cable installations. The program includes a steady-state and transient cable ratings solver that pertains to the analytical techniques described by Neher-McGrath and the IEC 287 and IEC 853 international standard. More CYMCAP information is provided in section 1.7.

3.1 Input Parameters in CYMCAP

The input parameters in CYMCAP are necessary to perform cable rating calculations. The input parameters include are the following:

3.1.1 Cable Component Parameters

The underground cable has been modeled by specifying the thickness of cable components such as conductor, conductor shield, insulation, insulation screen, sheath, concentric neutral wires and jacket. These cable parameters were taken from the *SRP 69 kV Underground System, Policy Procedures and Standards* book.

3.1.1.1 Conductor

The conductor material could be copper, aluminum or another user defined material. Voltage level, circular mil area, thickness and conductor diameter need to be provided as well. Conductor construction, for example, solid, round stranded, compact or compressed, segmental and hollow core are supported by CYMCAP.

3.1.1.2 Insulation

Insulation materials available in this program include Butyl rubber, EPR, PVC, Polyethylene and XLPE. If the insulation screen is made of semi-conducting material, the insulation screen will be considered as part of the insulation.

3.1.1.3 Insulation Shield

The insulation shield is commonly used as a semi-conducting layer over the insulation to create radial electrical stresses between the conductor and electrical ground. This means the electric field points outwards from the conductor in a uniformly radial manner. Each concentric circle between conductor and insulation shield represents an equipotential (isothermal) surface. If an insulation shield is modeled, CYMCAP will assume its material to be the same as insulation material.

3.1.1.4 Concentric Neutral Wires

CYMCAP provides flexibility in selecting the wire size and material, and the number of wires and length of lay. The length of lay is the longitudinal distance required for a particular tape to make one revolution around the previous layers. Ten times the previous layer's diameter has been used as the default length of lay in CYMCAP.

3.1.1.5 Outer Jacket

Outer jacket serves as the non-metallic covering which protects the underground cables against mechanical and chemical damages. The jacket is modeled in CYMCAP by specifying the thickness of the jacket insulation and jacket material. A number of materials including rubber sandwich, polychloroprene, polyethylene, PVC, and butyl

rubber are available in CYMCAP. Figure 3.1 illustrates all cable layers modeled in CYMCAP.

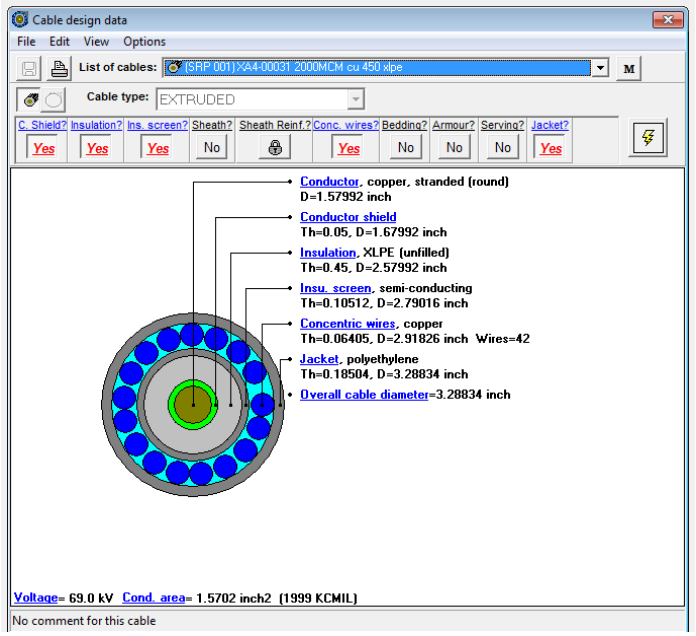

Fig. 3.1 Cable Modeling in CYMCAP

3.1.2 Duct Bank Dimension and Material Property Parameters

The fluidized thermal backfills (FTB) are utilized surrounding the cable conduits in the duct bank to achieve lower thermal resistivity and greater structural strength. The vertical and horizontal dimension of the duct bank and the thermal resistivity of the duct bank material are necessary to define (see Fig. 3.2).

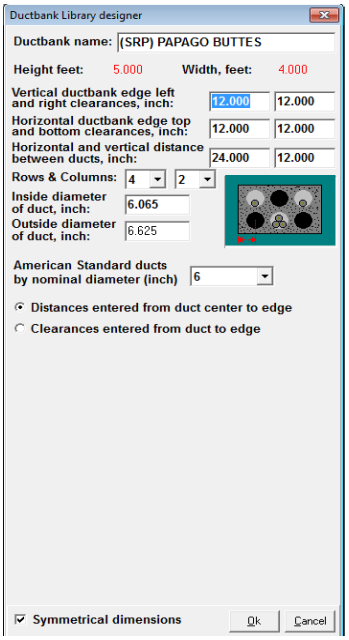

Fig. 3.2 Duct Bank Modeling in CYMCAP

3.1.3 Thermal Backfill Dimension and Material Property Parameters

Thermal backfill is put at the top of duct bank. The backfill is modeled by specifying the vertical and horizontal distance and thermal resistivity of the backfill material.

3.1.4 Ambient Temperature and Maximum Conductor Temperature

Ambient temperature is the soil ambient temperature. The maximum conductor temperature is specified into two distinctive values: the maximum conductor temperature allowable under steady state and transient rating operation.

3.1.5 Load curve

The load curves are essential for cable transient analysis. The user can define the load curve profile in load curve library. The load curve library is a database containing the description of various patterns of current as a function of time.

3.1.6 Heat Sink and Heat Source

Since the heat source or sink (i.e. adjacent water irrigation pipes, or even a canal bank) is considered to influence the cable ampacity. It is essential to model all heat sources/sinks nearby the underground cable properly. However, the diameter of heat source that a user can define in CYMCAP has to be less than 19 inches.

3.2 Assumptions of SRP 69 kV Cable Systems

To better illustrate the SRP cable rating computation input parameters, several assumptions for SRP 69 kV underground cable systems have been made.

3.2.1 Ambient Temperature

Although 25 ^{0}C has been selected as the default ambient temperature in CYMCAP, the ground temperature in Phoenix area is higher than the default value. To better represent the ground temperature in Phoenix, 35 ^{0}C was selected as the ambient temperature for all projects.

3.2.2 Maximum Conductor Temperature

Cross-linked polyethylene (XLPE) cables are used in SRP 69 kV underground systems. The maximum allowable steady-state operating temperature of XLPE is 90 ^{0}C. At this maximum temperature, the rate of consumption of the anti-oxidant has been calculated to provide a cable life of a minimum of 30 years. Therefore, the temperature rating in steady state calculations is 90 ^{0}C. Maximum conductor temperature under 300 hour emergency rating is 105 ^{0}C.

3.2.3 Thermal Resistivity

The thermal resistivity of soil and backfills employed by SRP are listed as following

Table 3.1 Thermal Resistivity for Soil and Backfills

Soil type (Stock Code No.)	Slurry type	K·m/W
Native Soil	N/A	1.20
Backfill (00-0104)	Controlled Low Strength 1/2 sacks of cement per cy	1.55
Backfill (00-0105)	Controlled Low Strength 1 sacks of cement per cy	1.05
Backfill (00-0106)	Controlled Low Strength 1-1/2 sacks of cement per cy	0.95

Note: * Thermal backfill has been used to improve the heat transfer between the cables and surrounding soil, resulting in current rating of cables increase. The cable ampacity enhancement has been achieved by the low thermal resistivity of backfill material.

3.2.4 Water Temperature in Arizona Canal

In Papago Buttes-Scottsdale 69 kV underground line, a portion of underground wires are installed underneath the Arizona Canal. It is difficult to get water temperature in this area. For the city of Tempe, the government website says that the average lake temperature during summer is 28 ^{0}C (82 ^{0}F) [11].

3.2.5 Load Factor

In *69 kV Underground Systems, Policy Procedures and Standards* book, load factors for each project are given as 75%. However, the load factors in the Papago

Buttes-Scottsdale 69 kV line and Beeline-Pico 69kV line are 85% and 90%, respectively. Since high load factors would result in ampacity de-ratings, the potential of the underground cable might not be fully used. It becomes apparent that the high load factor should be verified before being used. So the load factor of Papago Buttes-Scottsdale was calculated based on its historical loading. Because the high load factor occurs during the peak load period, the range for the load factor calculation was selected during peak load times (summer time into fall) from 2006 to 2012. The average current of the conductor was calculated for 300 hours (12.5 days) over the peak loading period, along with finding the maximum current during those 12.5 days. Note that the load factor was generated taking the transfer factor (transfer factor is defined in section 2.2 into account. The load factor in this period is the ratio of average current value to peak current.

$$LF_i = \frac{Avg_i}{Peak_i} \tag{3.1}$$

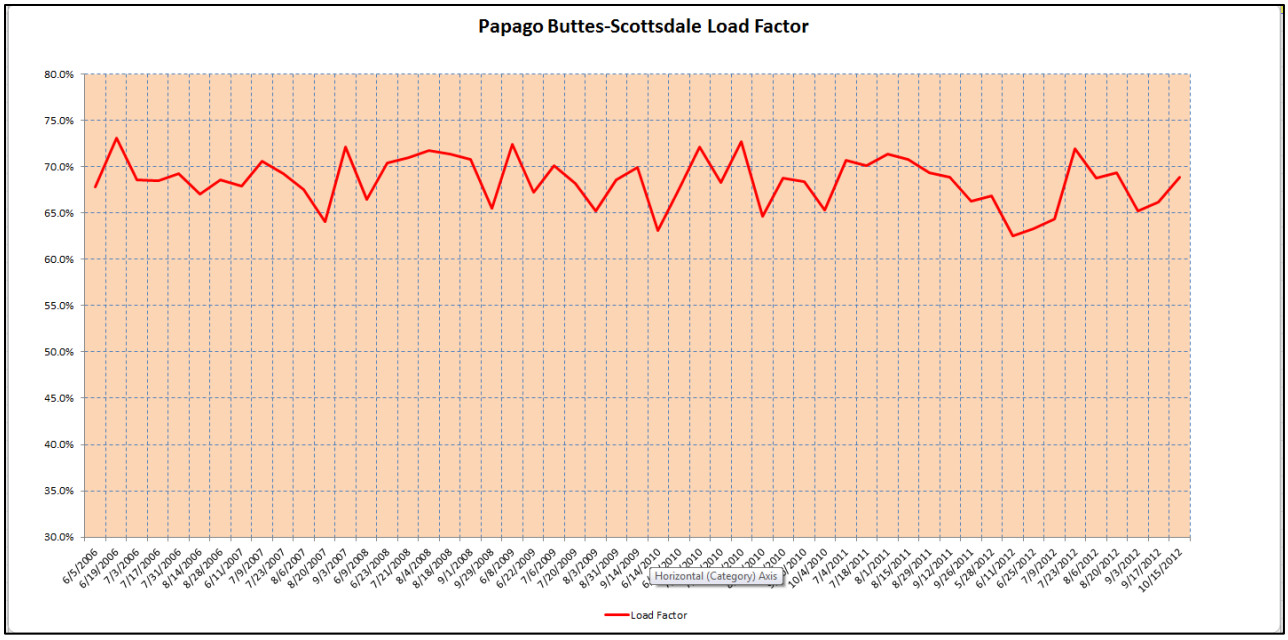

Fig. 3.3 Load Factor Calculated for Each Peak 12.5 Days (2006-2012)

for Papago Buttes-Scottsdale 69 kV Line

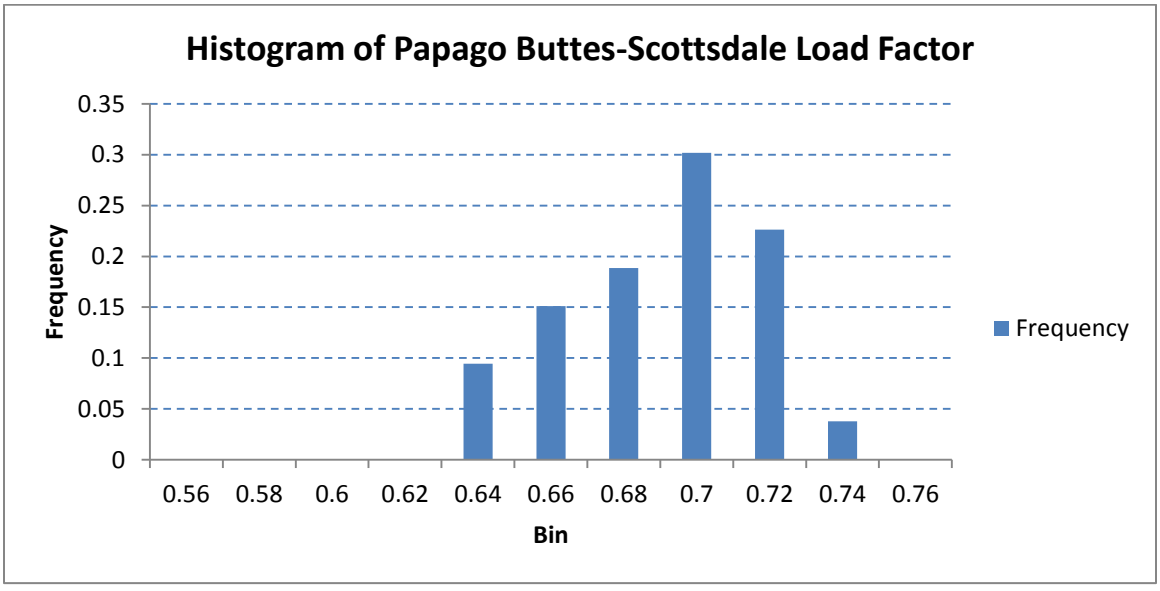

Fig. 3.4 Papago Buttes-Scottsdale Load Factor Frequency Distribution

From Fig. 3.4, this histogram was created to visualize the frequency distribution of the load factors for Papago Buttes-Scottsdale line. The majority of the load factors fell

between 0.685 and 0.715. Therefore, the original load factor of 85% is found to not be appropriate. In order to conservatively calculate the ratings for Papago Buttes-Scottsdale, a load factor of 75% was selected. This is better aligned with the other load factors shown in the *SRP 69 kV Underground System, Policy Procedures and Standards* book.

The same methodology was used verifying the load factor for the Beeline-Pico 69 kV line. The histogram in Fig. 3.6 summarizes the load factor at Beeline-Pico from 2006 to 2012 shown in Fig. 3.5. It indicates that the majority of load factors fell between 0.685 and 0.725. Since the frequency of load factor at Beeline-Pico line mostly fell between 68% and 72%, 75% was selected as an appropriate conservative load factor for the study.

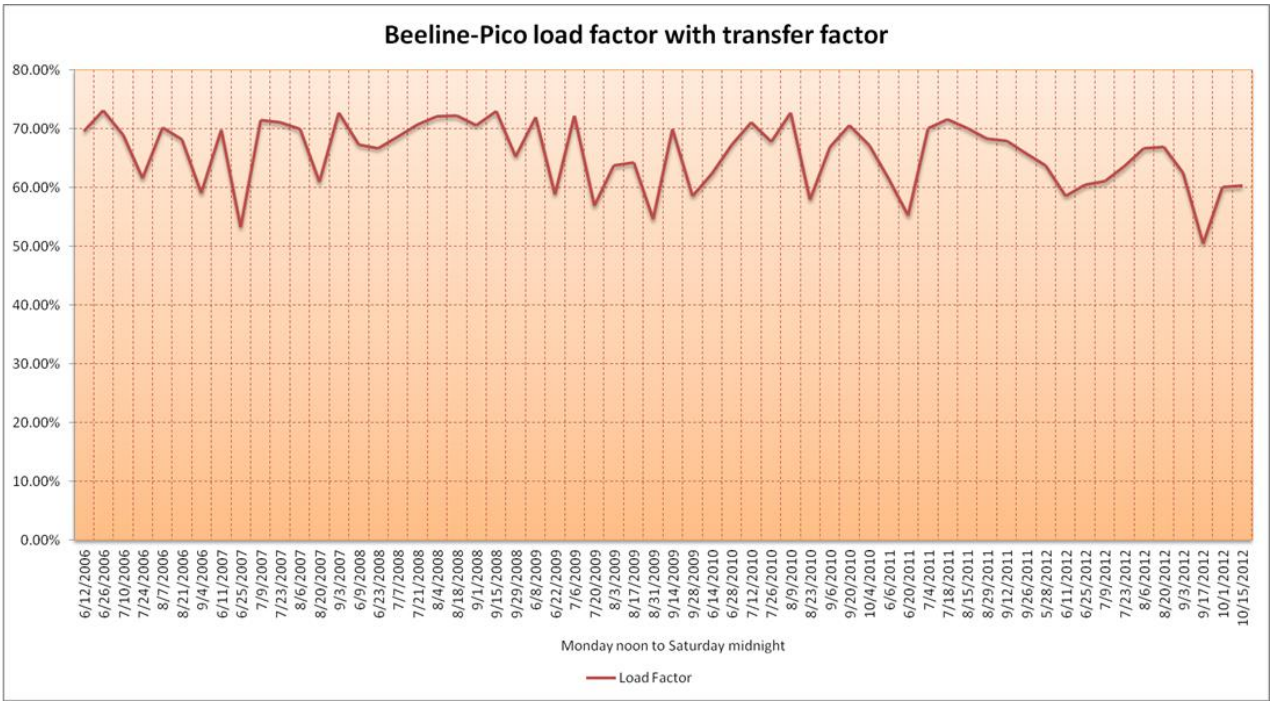

Fig. 3.5 Load Factor Calculated for Each Peak 12.5 Days (2006-2012)
for Beeline-Pico 69kV line

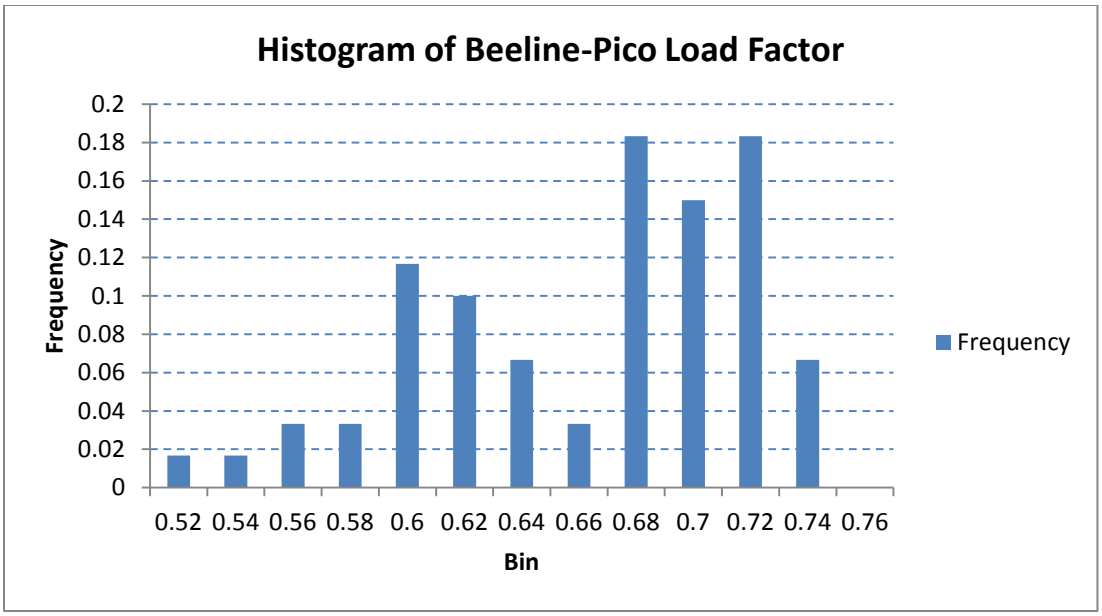

Fig. 3.6 Beeline-Pico Load Factor Frequency Distribution

3.2.6 Cable Depth

SRP 69 kV underground Systems, Policy Procedures and Standards book gives the depth of the cable installations for each project. In CYMCAP, the cable depth is defined as the distance from the surface of the earth to the top of the duct bank.

3.3 CYMCAP Steady State Rating Analysis

After creating the cable and duct bank model, the cable rating calculations can be performed by importing the cable and duct bank information from the CYMCAP cable library and duct bank library respectively. In steady state analysis, the ampacity is obtained by specifying the maximum conductor temperature of 90 ^{0}C. The thermal resistivity of fluidized thermal backfills surrounding the conduits, fluidized thermal backfill on the top of ductbank and thermal rho of native soil must also be known. Fig. 3.7 shows the graphical cable installation and steady state rating for each cable.

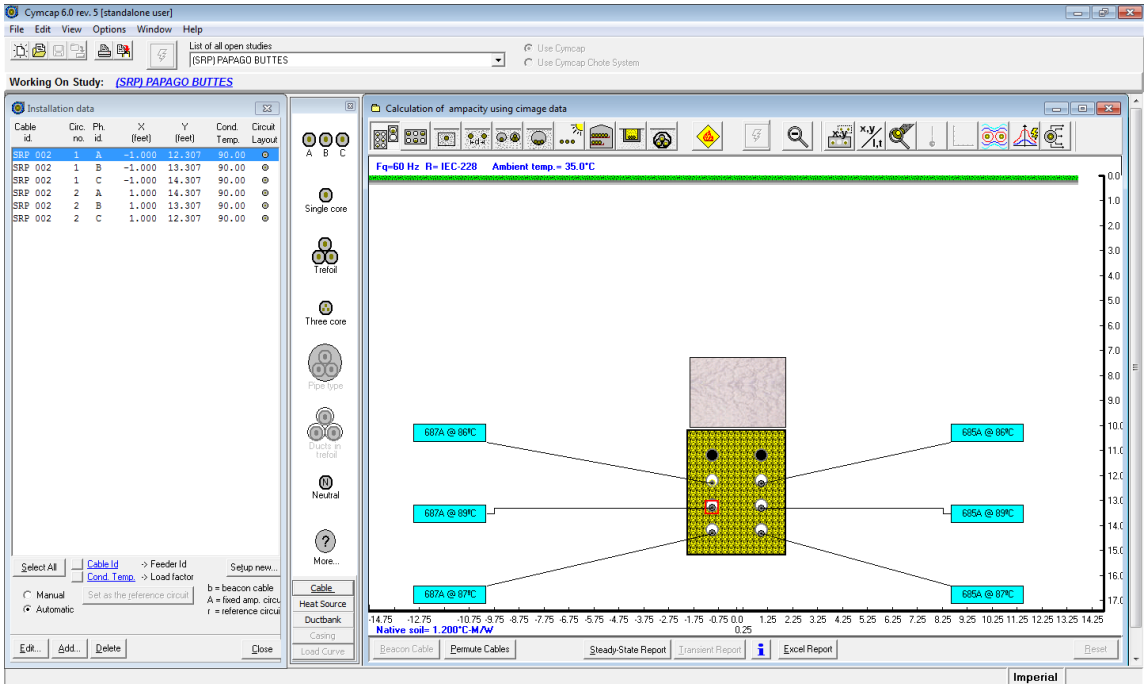

Fig. 3.7 CYMCAP Steady State Simulation

3.4 CYMCAP Transient Rating Analysis

Transient ratings are designed to allow the cables to carry a given amount of load for a specified period of time. The transient ratings, in this thesis, consist of a 100-hour emergency rating and a six-hour emergency rating. The calculation of transient ratings requires an iterative procedure. After each iteration, the cable loading is adjusted such that the conductor temperature hits 105 ^{0}C at the end of specified period of time.

3.4.1 100-Hour Emergency Rating Calculation

Step 1: Find the starting point for the calculations

The emergency calculations must be performed based on a given starting point. For simplification purposes, all of the 100-hour emergency rating calculations used the same starting point temperature. The largest value of the maximum conductor temperature was

used as the starting point temperature. From Table 3.2, the maximum conductor temperature among those projects is 44.83^{0}C. So the starting point for the 100-hour emergency calculation was set to 45^{0}C.

Table 3.2 Maximum Conductor Temperature in Each Line

Project	Emergency Period (7 days)	Critical Day	Maximum Temperature(^{0}C)
Papago Buttes-Scottsdale	07/11/09 - 07/17/09	07/14/09	44.83
Beeline-Pico	09/17/05 - 09/23/05	09/21/05	41.11
Big Spinner-Roe	08/28/12 - 09/03/12	09/02/12	43.54
Display 69 kV Tap	07/22/12 - 07/28/12	07/22/12	35.06
Clemans-Omega	09/14/08 - 09/20/08	09/20/08	35.36
McMullin-Wheeler	07/14/10 - 07/20/10	07/19/10	37.14
Gila-Austin	02/10/05 - 02/16/05	02/14/05	40.45
Falcon-Chopper	08/25/04 - 08/31/04	08/31/04	39.68
Rio Verde-Wheeler	12/14/07 - 12/20/07	12/15/07	37.43
Brandow-Pickrell	08/18/07 - 08/24/07	08/24/07	43.23
Anderson-Irvin	07/01/08 - 07/07/08	07/02/08	38.34
Hanger-Houston	10/04/12 - 10/10/12	10/10/12	37.27
Alameda-Ward	07/20/06 - 07/26/06	07/24/06	39.18
Cooley-Williams	05/07/07 - 05/13/07	05/12/07	40.41
San Tan-Clark	08/23/12 - 08/29/12	08/28/12	40.61
San Tan-Greenfield	07/16/06 - 07/22/06	07/22/06	39.69

Step 2: Establish the 100 hour daily load curve. A per unit sinusoidal shaped curve has been used to model the daily load shown in Fig. 3.8. Since the load factor is 75% which discussed in section 3.2.5, the centerline of sinusoidal function was set to be 0.75.

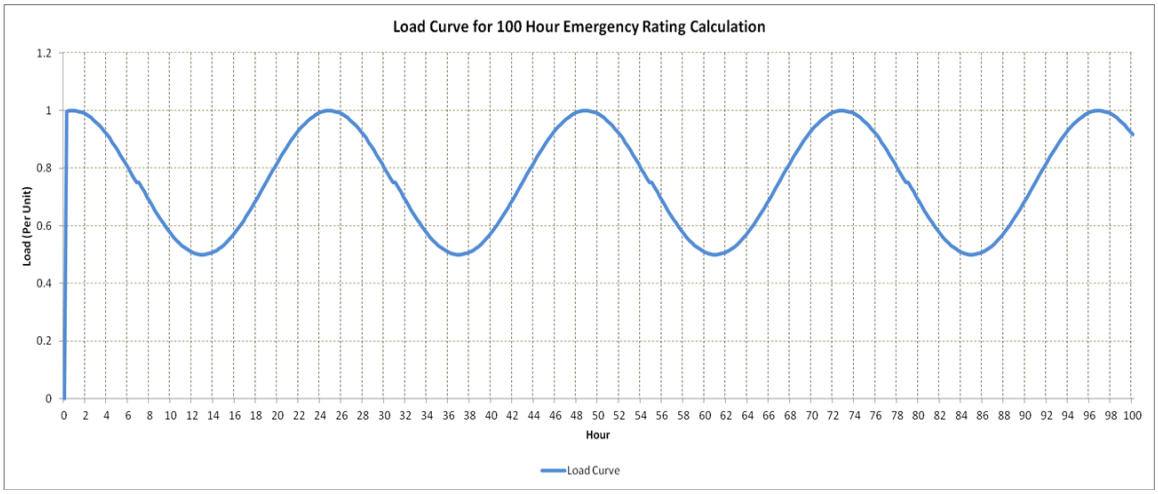

Fig. 3.8 100 Hour Daily Load Curve

Step 3: Run the CYMCAP transient analysis

As stated previously, an iterative method must be used to calculate the 100 hour emergency rating. The necessary steps are: Choose a number as the cable emergency rating and change that number in the transient data table in Fig. 3.9 until the temperature hits the 105 ^{0}C which is the maximum emergency temperature at 100th hour. This rating then becomes the 100 hour emergency rating.

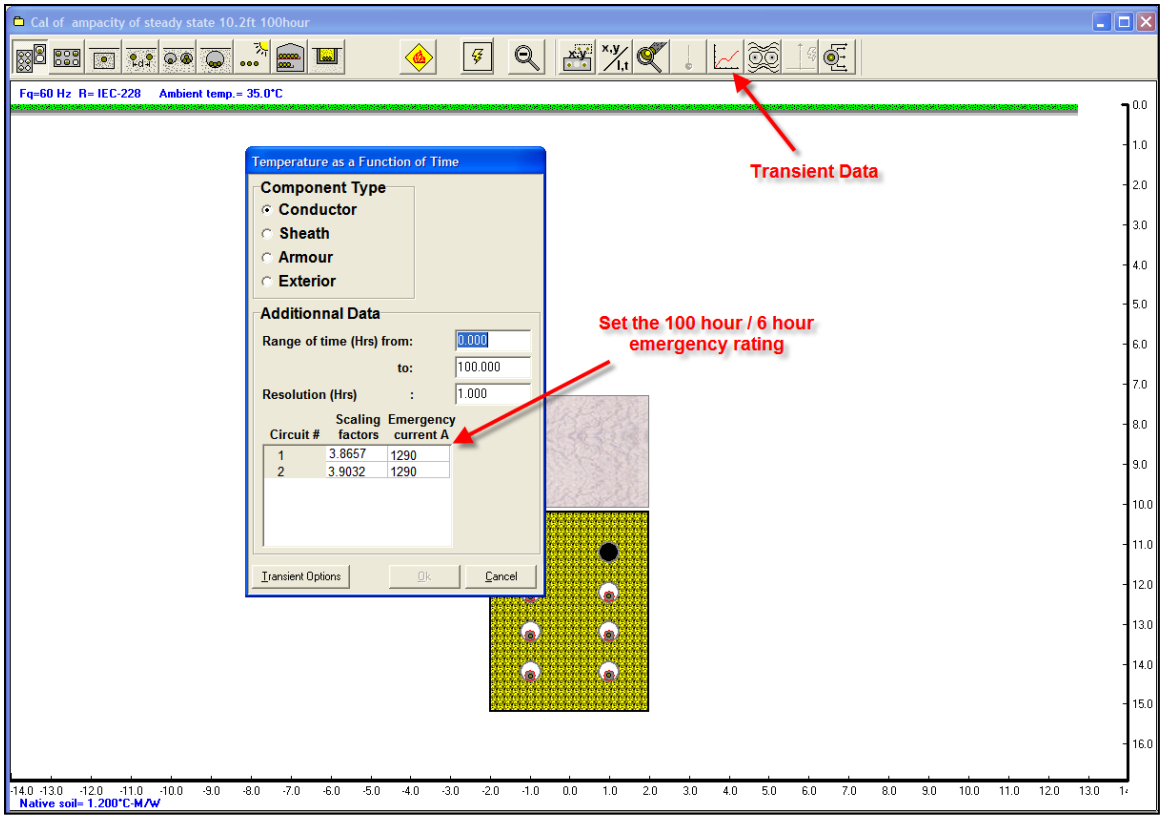

Fig. 3.9 Transient Data Table in CYMCAP

3.5 Result Summary

The steady state ratings of SRP underground lines have been created in Table 3.3. 2012 re-evaluated ratings column consists of steady state ratings and 300 hour emergency ratings. The 300 hour emergency ratings were determined by performing steady state rating calculations while using an increased maximum allowable conductor temperature of 105 ^{0}C.

In the existing rating columns, the load factors of Papago-Buttes-Scottsdale and Beeline-Pico are 85% and 90%, respectively. For other remaining projects, 75% was selected as the load factor. After taking load information from EMS to determine the load

factor, the load factors for Papago Buttes-Scottsdale and Beeline-Pico were found to be 75%.

Comparing Table 3.3 with the historical ratings (which can be found in *SRP 69 kV Underground Systems, Policy Procedures and Standards* book,) the updated steady-state ratings were very close to the existing values. Due to the change of load factor in Beeline-Pico, the largest difference between the existing steady-state ratings and re-evaluated ones is 7.15% shown in Table 3.4.

Table 3.3 Existing Ratings vs Re-evaluated Ratings

	Existing Ratings			2012 Re-evaluated Ratings		
Cable Circuit	Load Factor	Steady State (A)	300 Hour Emergency Rating (A)	Load Factor	Steady State (A)	300 Hour Emergency Rating (A)
Papago Buttes-Scottsdale	85%	1400	1800	75%	1490	1657
Beeline-Pico	90%	825	970	75%	884	984
Big Spinner-Roe	75%	1550	1800	75%	1568	1794
Display 69 kV Tap	75%	900	1000	75%	931	1036
Clemans-Omega	75%	900	1000	75%	928	1033
McMulin-Wheeler	75%	1700	1900	75%	1674	1862
Gila-Linox-Austin-Air Park	75%	1550	1800	75%	1616	1798
Falcon-Chopper	75%	850	1000	75%	870	969
Rio Verde-Wheeler	75%	1700	1900	75%	1680	1868
Brandow-Pickrell Tap	75%	1600	1900	75%	1652	1836
Anderson-Irvin	75%	1700	1900	75%	1600	1736
Hanger-Houston	75%	1600	1900	75%	1604	1756
Alameda-Ward	75%	1700	1900	75%	1704	1898
Cooley-Williams	75%	1650	1800	75%	1640	1828
San Tan-Clark	75%	1700	1900	75%	1720	1916
San Tan-Greenfield	75%	1700	1900	75%	1720	1916
Hoopes Substation	N/A	N/A	N/A	75%	1538	1710

Table 3.4 Percent Difference Between Existing Ratings and Re-evaluated Ratings

	Existing Ratings			2012 Re-evaluated Ratings		
Cable Circuit	Load Factor	Steady State (A)	300 Hour Emergency Rating (A)	Load Factor	Steady State Difference	300 Hour Rating Difference
Papago Buttes-Scottsdale	85%	1400	1800	75%	6.43%	-7.94%
Beeline-Pico	90%	825	970	75%	7.15%	1.44%
Big Spinner-Roe	75%	1550	1800	75%	1.16%	-0.33%
Display 69 kV Tap	75%	900	1000	75%	3.44%	3.60%
Clemans-Omega	75%	900	1000	75%	3.11%	3.30%
McMulin-Wheeler	75%	1700	1900	75%	-1.53%	-2.00%
Gila-Linox-Austin-Air Park	75%	1550	1800	75%	4.26%	-0.11%
Falcon-Chopper	75%	850	1000	75%	2.35%	-3.10%
Rio Verde-Wheeler	75%	1700	1900	75%	-1.18%	-1.68%
Brandow-Pickrell Tap	75%	1600	1900	75%	3.25%	-3.37%
Anderson-Irvin	75%	1700	1900	75%	-5.88%	-8.63%
Hanger-Houston	75%	1600	1900	75%	0.25%	-7.58%
Alameda-Ward	75%	1700	1900	75%	0.24%	-0.11%
Cooley-Williams	75%	1650	1800	75%	-0.61%	1.56%
San Tan-Clark	75%	1700	1900	75%	1.18%	0.84%
San Tan-Greenfield	75%	1700	1900	75%	1.18%	0.84%
Hoopes Substation	N/A	N/A	N/A	75%	N/A	N/A

Table 3.5 100 and 6 hours Emergency Ratings

Project	100 Hour Emergency Rating (Amps)	6 Hour Emergency Rating (Amps)
Papago Buttes-Scottsdale	2580	3000
Beeline-Pico	1330	1510
Big Spinner-Roe	2660	3020
Display 69 kV Tap	1340	1520
Clemans-Omega	1340	1520
McMullin-Wheeler	2640	3020
Gila-Linox-Austin	2600	3000
Falcon-Chopper	1320	1500
Rio Verde-Wheeler	2660	3020
Brandow-Pickrell	2620	3160
Anderson-Irvin	2480	2960
Hanger-Houston	2480	2980
Alameda-Ward	2960	3460
Cooley-Williams	2800	3440
San Tan-Clark	2820	3440
San Tan-Greenfield	2820	3440

4 MATHMATICAL MODELS FOR CABLE RATING PREDICTION

Regression is a statistical method to explore the relationship between a response variable and one or more predictor variables. In this thesis, regression analysis has been used to predict SRP 69 kV underground cable steady state ratings. The regression methods include linear regression and nonlinear regression. The nonlinear regression approaches consist of two types of expressions: multiple logarithm terms and mixture of exponential and logarithm terms.

4.1 Problem Definition

Six single core cables are installed within a four-foot wide, five-foot high concrete duct bank (see Fig. 4.1). The left three conductors consist of a three phase circuit, the right ones consist of another parallel circuit. All of the conductors are installed in conduits with inner and outer diameter equals to 6.065 inches and 6.625 inches, respectively. The ambient temperature is assumed to be 35 ^{0}C. The maximum allowable conductor temperature has been set to 90 ^{0}C.

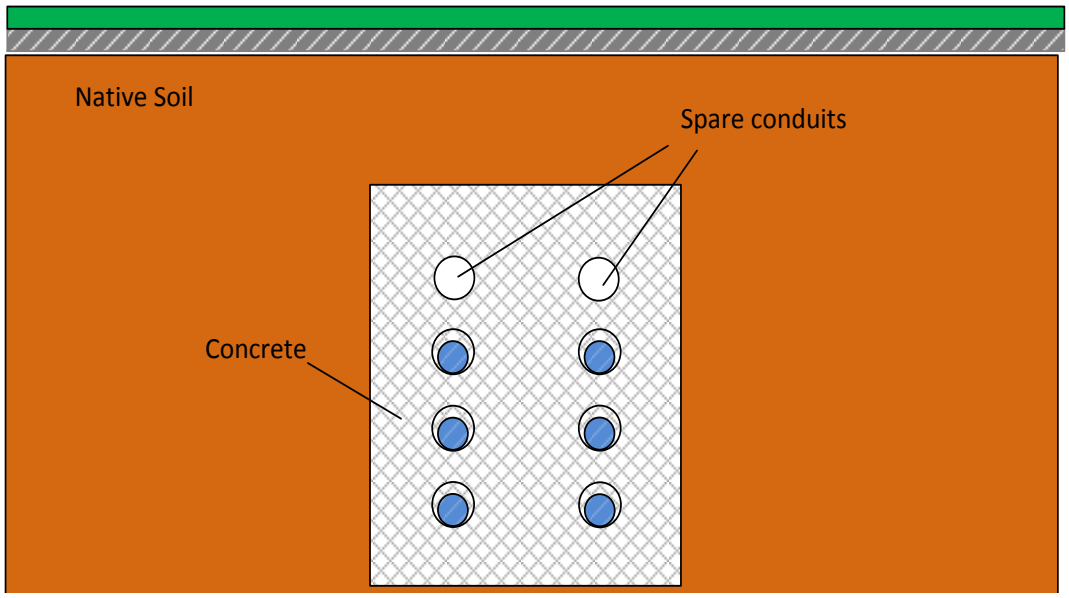

Fig. 4.1 Illustration of Cable Configuration

4.2 Data Gathering and Preparation

The data used to create the regression models is called training data. A training dataset has been built based on a typical range of predictor variables. After the model being built, we need to find the accuracy of the model fit. Apparently, the model will be optimistically estimated, if using the training data itself in the testing process. Thus, we can get realistic estimate of the model with unseen data which is different from the training dataset. The unseen data is widely known as the validation dataset. A sample of 70 data points is generated as the training data using CYMCAP to calculate the ampacities (APPENDIX I). In terms of validation data, 80 data points have been chosen to test the regression models ability to predict accurate ampacities (APPENDIX II).

Since the cable ampacity is primarily influenced by cable installation conditions and its material characteristics, each training data point or validation data point includes

the conductor size, the duct bank thermal resistivity, the soil thermal resistivity and the depth for cable installations.

4.3 Model Building and Model Evaluation

4.3.1 Linear Regression

Linear regression is the most commonly used technique to construct a linear best-fitting function for the observed data. The predictor variables include four independent variables: the cable size x_1, the thermal resistivity of duct bank x_2, the thermal resistivity of native soil x_3, and the depth from the surface of the earth to the top of the ductbank x_4. The purpose of linear regression is to determine the steady state cable rating y which is affected by changes in other predictor variables. The relationship between the response variable and the predictor variables can be formed as follows

$$y = \beta_1 x_1 + \beta_2 x_2 + \beta_3 x_3 + \beta_4 x_4 + \beta_5 + \varepsilon \tag{4.1}$$

where ε is a random error term, β_i (i=1, 2, 3, 4, 5) are the prediction coefficients. However, the values of β_i (i=1, 2, 3, 4, 5) are unknown. The method to obtain the estimates of β_i (i=1, 2, 3, 4, 5) is to minimize the sum of the squares of the errors in (4.2) [12]:

$$S = \sum_{i=1}^{n} \varepsilon_i^2 = \sum_{i=1}^{n} (y - \beta_1 x_{1,i} - \beta_2 x_{2,i} - \beta_3 x_{3,i} - \beta_4 x_{4,i} - \beta_5)^2 \tag{4.2}$$

The least squares estimates of β_i (i=1, 2, 3, 4, 5) are written as b_i (i=1, 2, 3, 4, 5). Coefficients b_i (i=1, 2, 3, 4, 5) can be computed by taking the partial derivatives of S with respect to β_i (i=1, 2, 3, 4, 5) and set each equation to be zero. Replace β_i (i=1, 2, 3, 4, 5)

with b_i (i=1, 2, 3, 4, 5) because the values obtained by minimizing the sum of squared errors are not the true coefficients, β_i, but estimates of the true coefficients, b_i. Then the linear regression model is

$$\hat{y} = b_1 x_1 + b_2 x_2 + b_3 x_3 + b_4 x_4 + b_5 \tag{4.3}$$

where $\hat{y}$ are the predicted values. The predicted values can be calculated by substituting pairs of the dataset x_i (i=1, 2, 3, 4). The discrepancy between the actual value of response variable y and the predicted value $\hat{y}$ is called residual shown in Equation (4.4) [12]

$$e_i = y_i - \hat{y}_i \tag{4.4}$$

Seventy selected data points have been used as the training data. These sampled data can be found at Appendix I. The prediction formula coefficients b_1, b_2, b_3, b_4, b_5 can be calculated by MATLAB which is shown in Table 4.1.

Table 4.1 Formula Coefficient Calculated by Linear Regression Using 70 Training Data

Coefficient	Value
b_1	0.3985
b_2	-132.8848
b_3	-266.7356
b_4	-21.4610
b_5	1533.2404

4.3.2 Model Evaluation

An effective way to check the adequacy of regression models is to produce the residual plots. The residual plot is a graph of the residuals against the predicted variables. The prediction residual is $e_i = y_i - \hat{y}_i$. A decent prediction model should be well behaved such that the residuals are randomly distributed around zero in the residual plots.

However, from the residual plot in Fig. 4.2, the residual pattern trends to decrease at first and increase as the predicted value rises. This indicates that the model needs non-linear terms. For example, the exponential or logarithm terms may be necessary. The largest residual obtained by the training data and the validation data are -7.33% in Fig. 4.2 and 21.24% in Fig. 4.3, respectively.

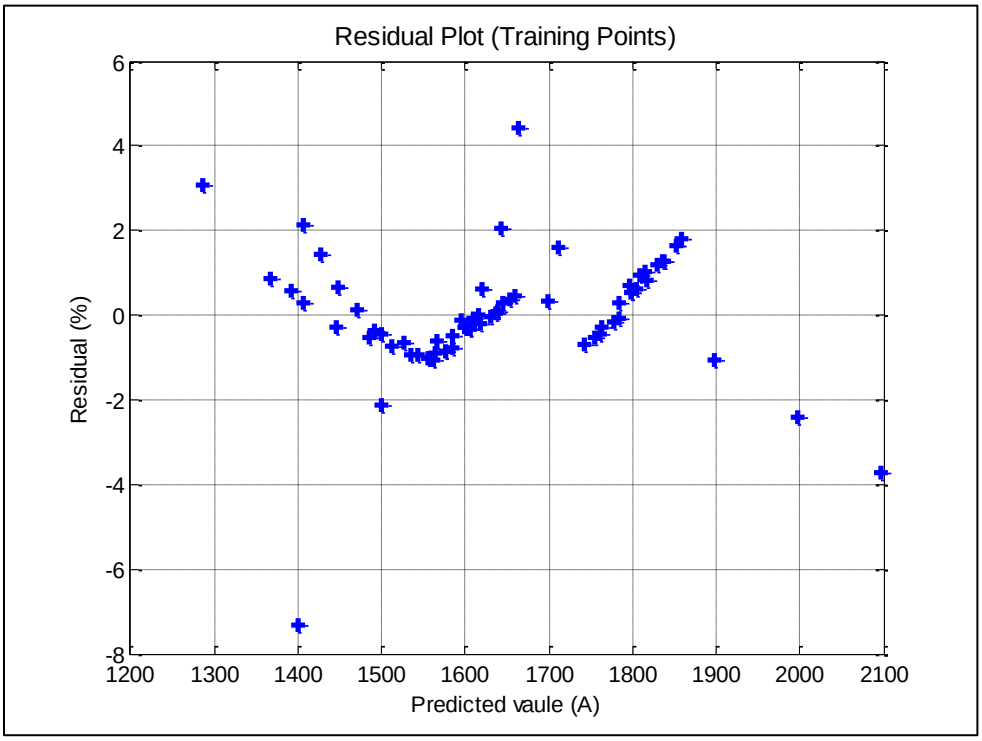

Fig. 4.2 Linear Model Residual Plot (Training Dataset)

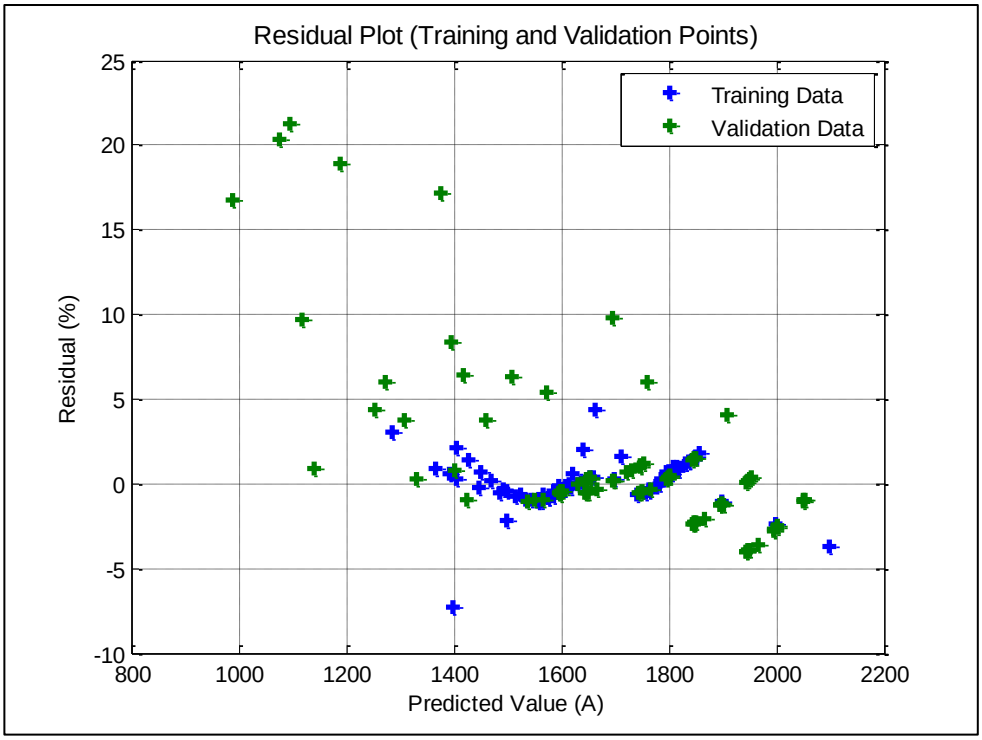

Fig. 4.3 Linear Model Residual Plot (Training and Validation Dataset)

The residual duration curves for the training dataset and the validation dataset are shown in Fig. 4.4 and Fig. 4.5. The residual duration curves provide the statistical summary for the residuals. Fig. 4.5 shows there will be 10% chance to get 14% or higher residuals. It indicates that the linear model cannot adequately summarize the relationship between the variables. Therefore, a linear model is inappropriate.

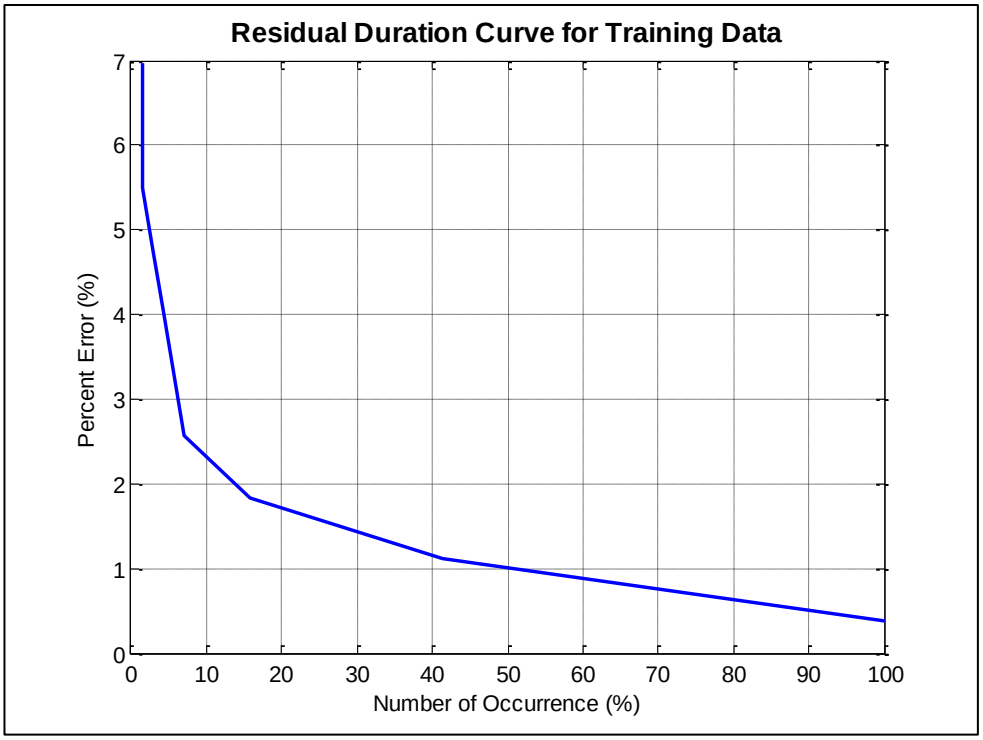

Fig. 4.4 Linear Model Residual Duration Curve (Training Data)

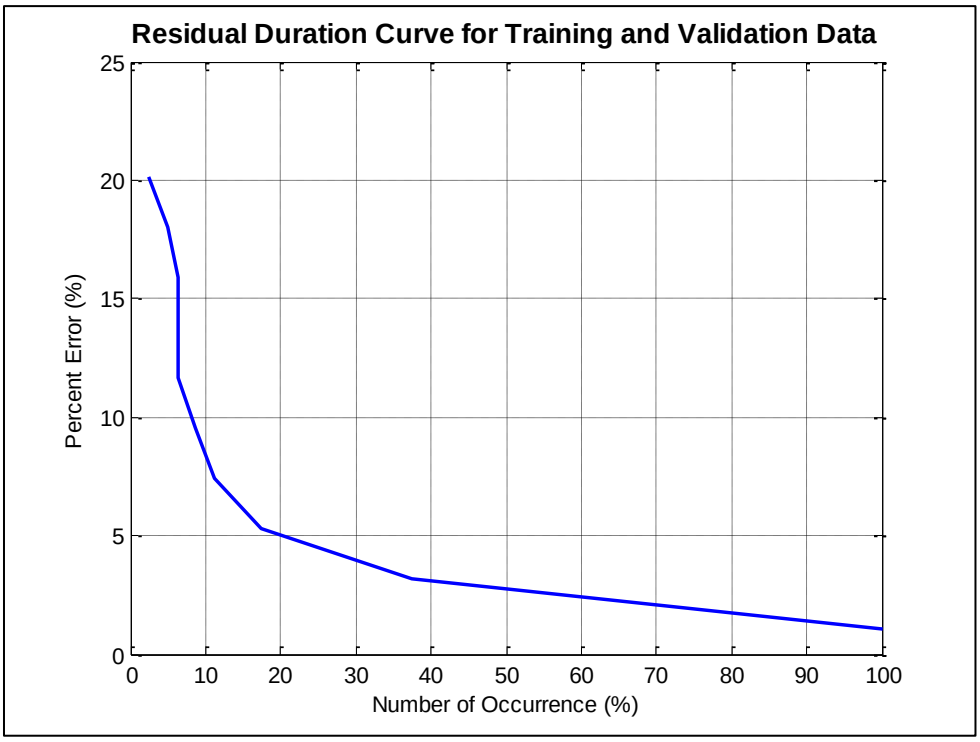

Fig. 4.5 Linear Model Residual Duration Curve (Training and Validation Data)

4.3.3 Nonlinear Regression with Multiple Logarithmic Terms

The regression analysis is always started with the assumption of a linear relationship between the response variable and the predictor variables. However, there are many problems in engineering where the relationships cannot be fitted to a linear model and hence it is more appropriate to develop an expression through nonlinear regression. There are two popular nonlinear equation forms:

$$y = ae^{x} \tag{4.5}$$

$$y = a\log(x) \tag{4.6}$$

The nonlinear regression model can be built based on an exponential growing or shrinking equation, thus the Equation (4.5) is obtained. Additionally, the response variable may grow or shrink logarithmically which is shown in Equation (4.6). In this section, the regression model is created based on the following assumptions:

1. The steady state rating of the underground cable ($\hat{y}$) increases when a larger cable size (x_1) has been used.

2. The steady state rating ($\hat{y}$) decreases when a surrounding backfill with higher resistivity (x_2) or a higher native soil resistivity (x_3) has been deployed.

3. The steady state rating ($\hat{y}$) decreases when the cables are put underground in a deeper depth (x_4)

The nonlinear model would like this:

$$\hat{y} = a x_1^{c_1} x_2^{c_2} x_3^{c_3} x_4^{c_4} \quad (4.7)$$

where $\hat{y}$ is the underground cable steady states rating, c_1 is expected to be positive, while c_2, c_3, c_4 are expected to be negative values.

To solve this nonlinear Equation (4.7), the common method is data transformation. Data transformation is simply means that the response variable or predictor variable is represented in a transformed form by using a mathematical operation to change its measurement scale. The transformation of exponentiation is shown in the table below.

Table 4.2 Regression Equation Transformation

Original Function	Transformation	Transformed Function
$\hat{y} = ax^c$	$\hat{y}' = \log \hat{y}, c_0 = \log a$	$\hat{y}' = c \log(x) + c_0$

Take log on both sides of (4.7), it becomes

$$\log(\hat{y}) = c_1 \log(x_1) + c_2 \log(x_2) + c_3 \log(x_3) + c_4 \log(x_4) + \log a \quad (4.8)$$

Then the transformation has been applied to Equation (4.8),

$$\hat{y}' = c_1 \log(x_1) + c_2 \log(x_2) + c_3 \log(x_3) + c_4 \log(x_4) + c_5 \quad (4.9)$$

Where $\hat{y}' = \log(\hat{y})$, $c_5 = \log a$.

Equation (4.9) demonstrates that the nonlinear function has been linearized by using a logarithmic transformation. The advantage of the using data transformation is to convert the original nonlinear problem to a linear regression problem; this can be achieved by applying an appropriate transformation to one or multiple variables. A total of 70 data points have been used to perform the linear regression analysis. The regression

coefficients were obtained by minimizing the sum of the squares of the residuals. The results are shown in Table 4.3.

Table 4.3 Formula Coefficients Calculated by Linear Regression Using 70 Sampled Data

Coefficient	
c_1	0.4364
c_2	-0.1186
c_3	-0.2525
c_4	-0.0762
c_5	4.3223

From the results shown above, it confirms the assumption that c_1 is positive, and the other coefficients are negative.

4.3.4 Model Evaluation

From Fig. 4.6, the residuals are calculated based on the training data. As we can see that the worst residual in Fig. 4.6 is around -2%. The residual plot shown in Fig. 4.6 indicates that the logarithm model can fit the training data well. However, from the residual plot generated by the validation data in Fig. 4.7, the largest residual is approximately -7.97% which means the logarithmic model explains the validation data acceptably for engineering purposes, which is usually taken as accuracy to within 10%.

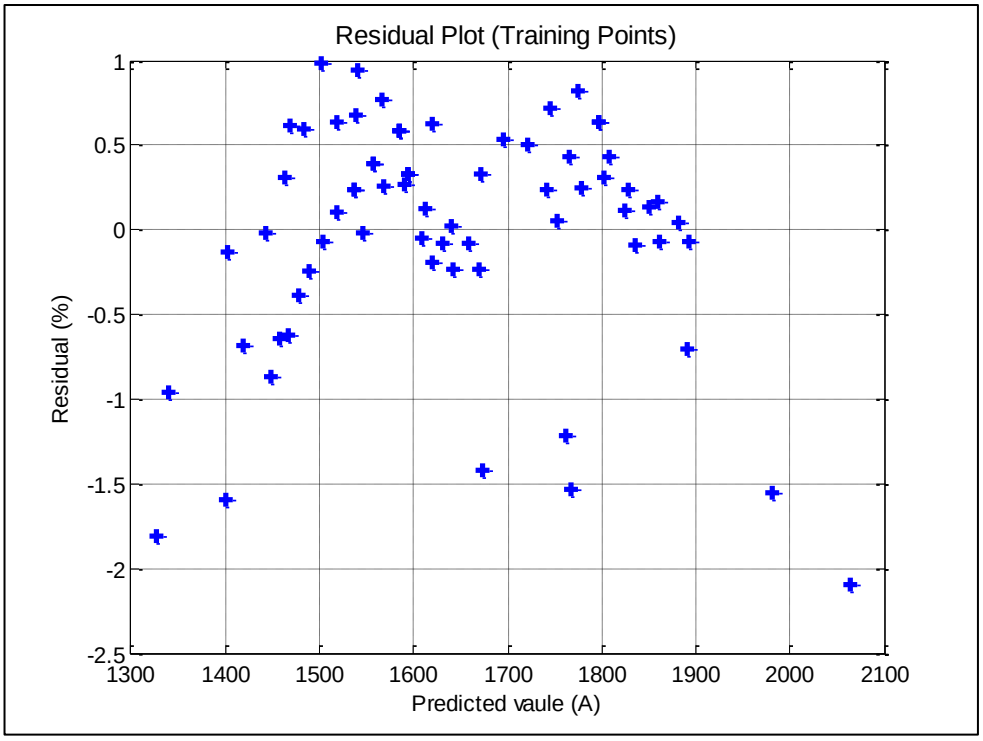

Fig. 4.6 Multiple Logarithm Model Residual Plot (Training Dataset)

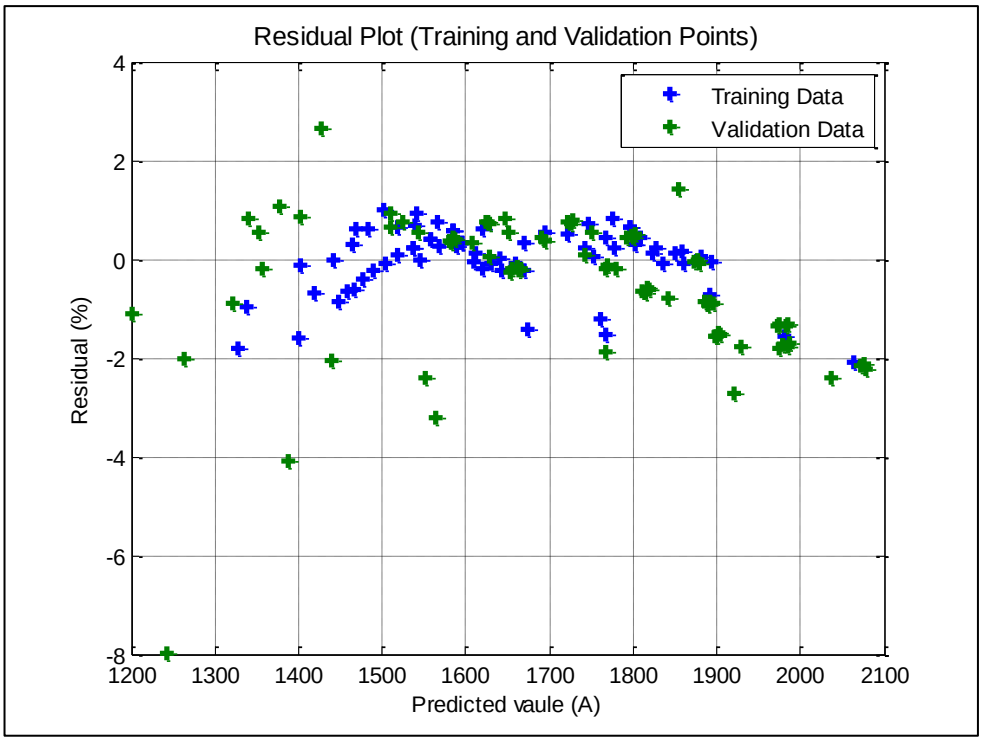

Fig. 4.7 Multiple Logarithm Model Residual Plot (Training and Validation Dataset)

The percent error plotted against the number of occurrences for training data and validation data are shown in Fig. 4.8 and Fig. 4.9. In Fig. 4.9, it is demonstrated that there is a 20% chance to get the residual of 2.2% or even higher.

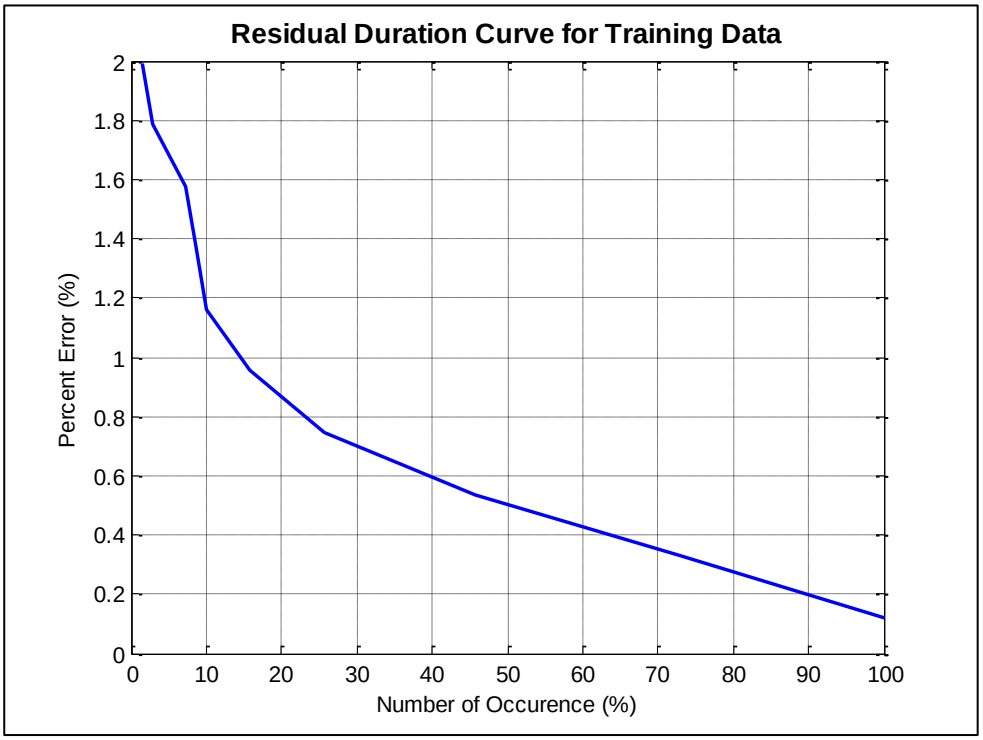

Fig. 4.8 Multiple Logarithm Model Error Duration Curve (Training Data)

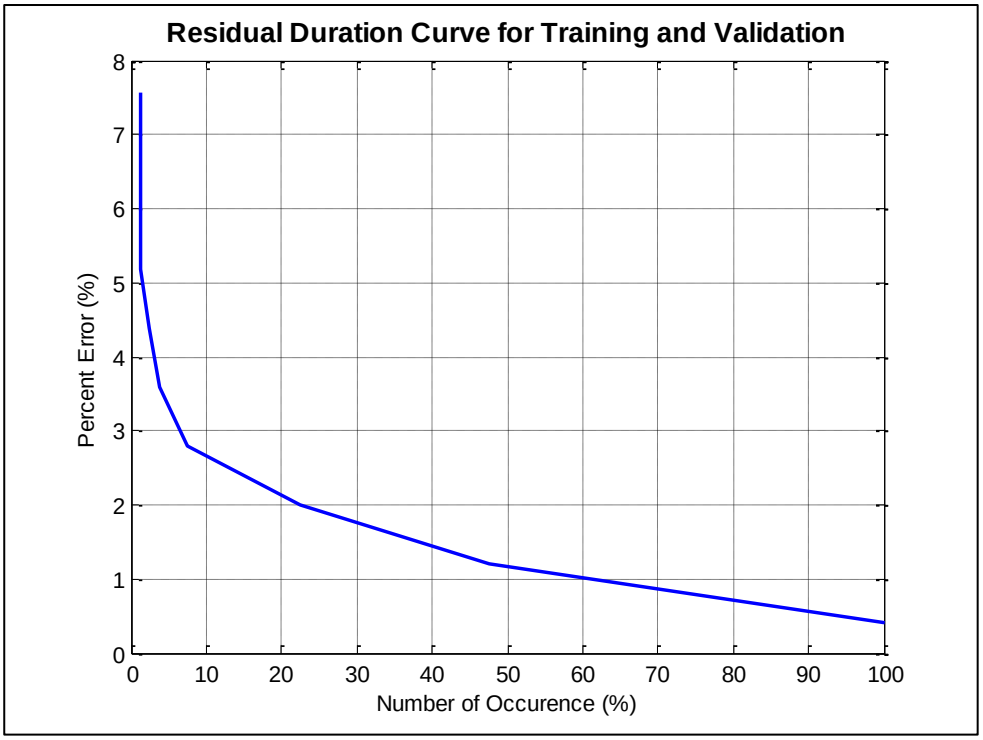

Fig. 4.9 Multiple Logarithm Model Error Duration Curve (Training and Validation Data)

4.3.5 Nonlinear Regression with Logarithmic and Exponential Terms

When the method with logarithm terms is applied in section 4.3.2, the gaps between observed values and predicted values remain acceptable, but there is a desire to see if this can be improved. Therefore, a new model, that includes logarithmic and exponential functions, is proposed as follows:

$$\hat{y} = k_1 x_1^{\,k2} + k_3 e^{k_4 x_2} + k_5 e^{k_6 x_3} + k_7 \log(x_4) + k_8 \qquad (4.10)$$

The coefficients are calculated using the least squares approach. The best-fit model is achieved when the sum of the squared residuals is minimized. MATLAB was used to perform the nonlinear model coefficients calculation. The prediction coefficients of the nonlinear regression were summarized in Table 4.4.

Table 4.4 Formula Coefficient Calculated by Logarithm and Exponential Model Using 70 Sampled Data

Coefficient	Values
k_1	245.9169
k_2	0.3047
k_3	691.4659
k_4	-0.2887
k_5	1095.2604
k_6	-0.7206
k_7	-123.1099
k_8	-1510.0346

4.3.6 Model Evaluation

Fig. 4.10 and Fig. 4.11 illustrate the residual plots for the model implemented with more nonlinear terms as logarithmic and exponential function. It can be seen from Fig. 4.10 that the large errors have been sufficiently eliminated. The worst residual turns out to be -1.53% shown in Fig. 4.10 when the training dataset is used as test data. The residual plot generated by the validation dataset in Fig. 4.11 shows that the gaps between observed values and predicted values have been reduced, compared with multiple logarithm method. The maximum residual is approximately 3.03% which has smaller errors than the logarithm model (-7.97%).

The residual duration curves are shown in Fig. 4.12 and Fig. 4.13, which also indicate the errors in this model have been reduced significantly. In Fig. 4.12, it shows that the residual is always smaller than 1.5% when the training data was applied as testing data. The residual duration curve in Fig. 4.13 demonstrates that the residual of training and validation dataset was never greater than 3%.

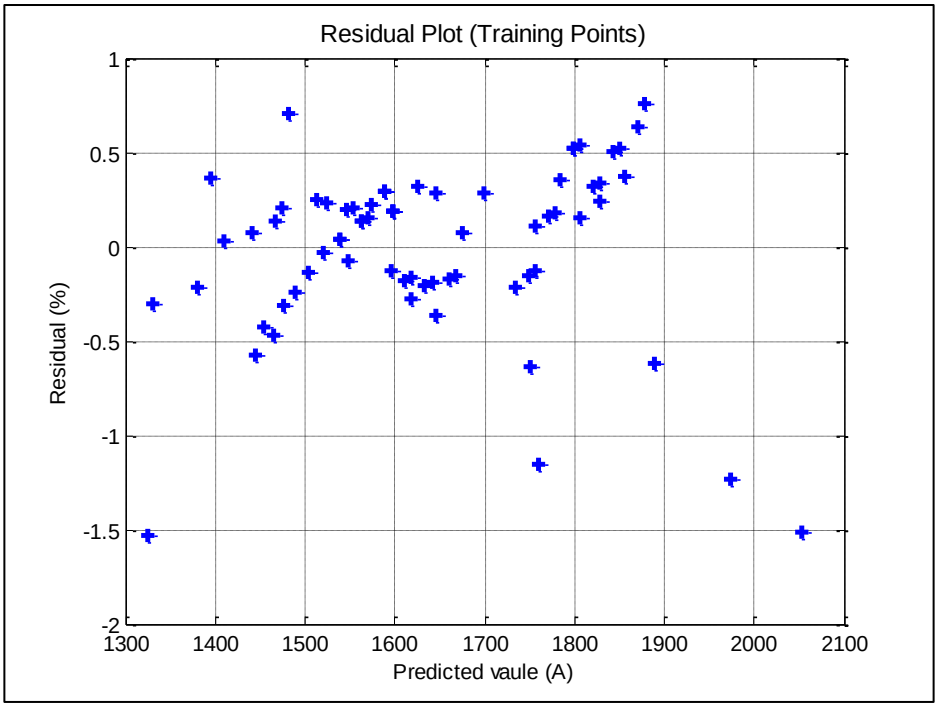

Fig. 4.10 Logarithmic and Exponential Model Residual Plot (Training Dataset)

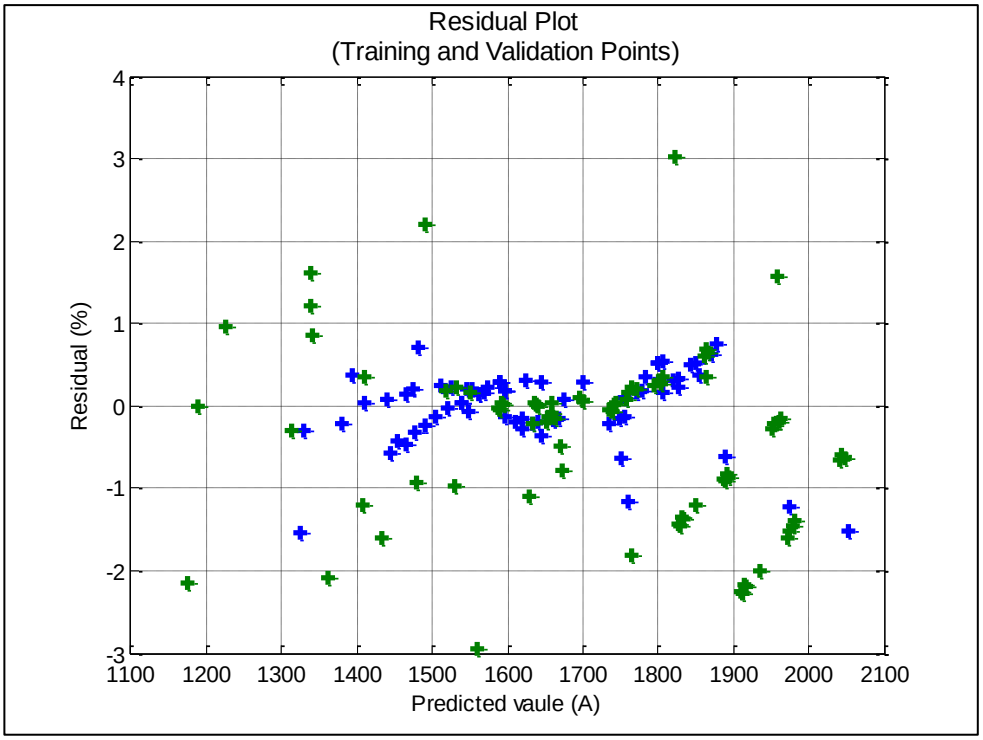

Fig. 4.11 Logarithmic and Exponential Model Residual Plot (Training and Validation Dataset)

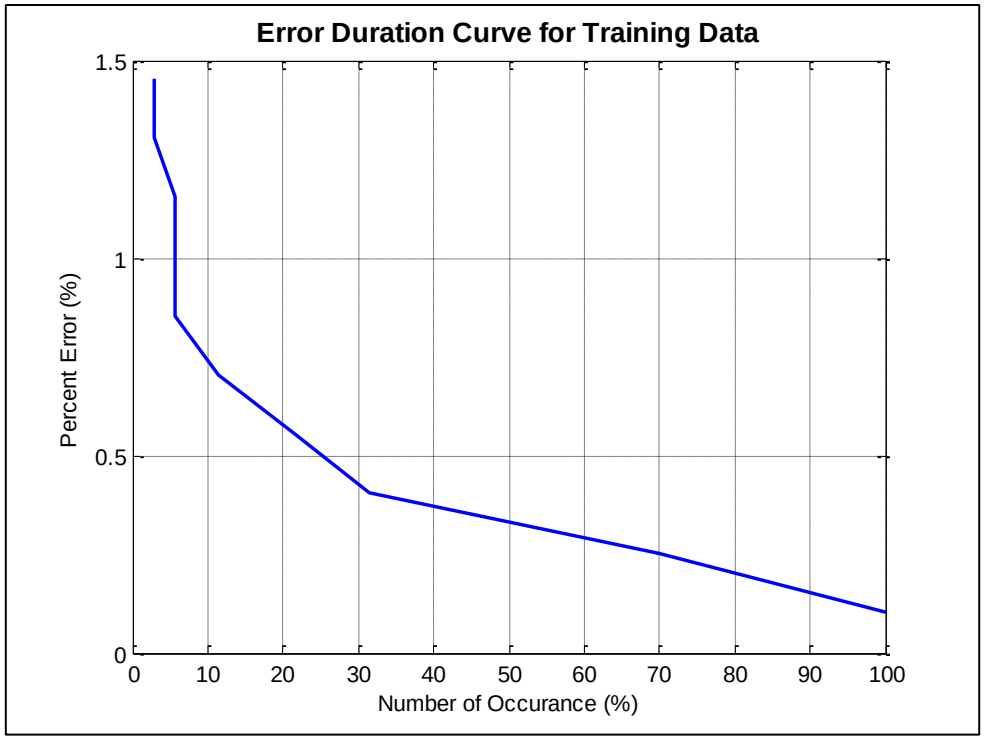

Fig. 4.12 Logarithmic and Exponential Model Error Duration Curve

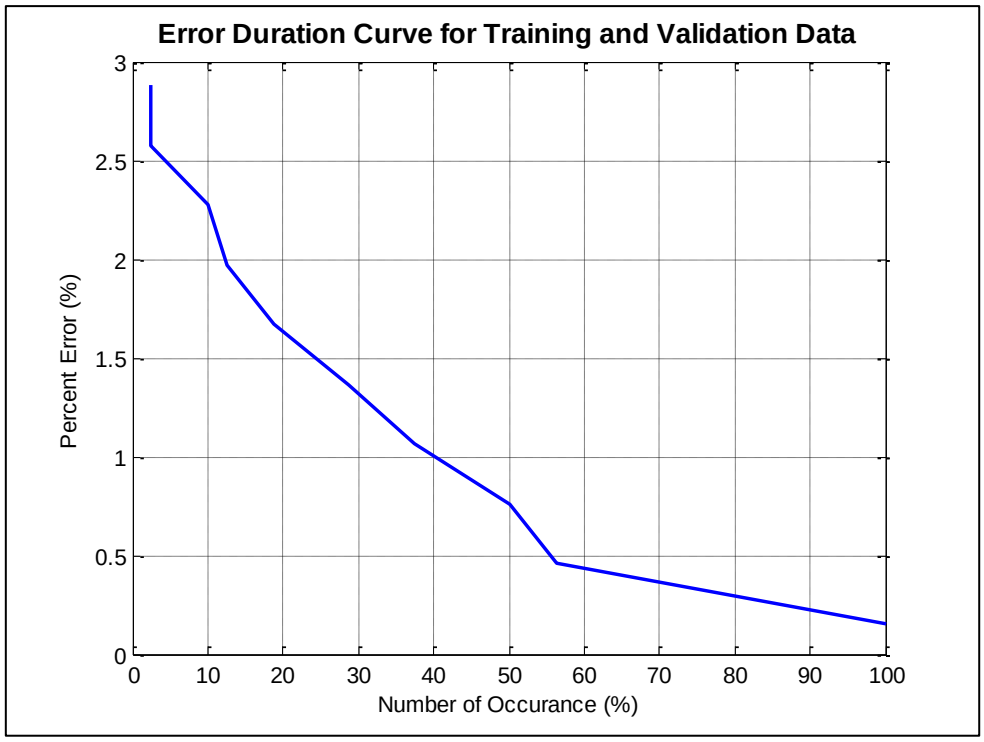

Fig. 4.13 Logarithmic and Exponential Model Error Duration Curve

4.4 Comparison of performance between three methods

The mean square errors were calculated for the linear regression model, logarithmic model, and mixture of the logarithmic and exponential models. Table 4.5 shows the mean square errors and maximum errors for three methods mentioned above.

Table 4.5 Mean Square Error and Maximum Percentage Error between three methods

	Mean Square Error		Maximum Percentage Error	
	Training Dataset (A^2)	Validation Dataset (A^2)	Training Dataset (%)	Validation Dataset (%)
Linear Regression	539.49	3874.64	-7.33	21.24
Logarithmic Model	127.74	377.18	-2.09	-7.97
Mixture of Logarithmic and Exponential Model	61.77	226.38	-1.53	3.03

4.5 Conclusion

Several regression models are introduced to investigate the relationship between underground cable steady state ratings and several predictor variables. The reliability of regression models were evaluated using, as metrics, mean square errors and maximum percentage errors. Applying the regression model with a mixture of logarithmic and exponential terms reduces the MSE from 127.74 to 61.77 (Table 4.5). Table 4.5 also shows a decrease in the maximum prediction error from -2.09% to -1.53% in training dataset. In terms of the maximum percent error shown in Table 4.5, the worst error in the mixture of logarithmic and exponential model is only 3.03% which is significantly decreased from linear method (21.24%). Based on these observations, the mixture of logarithmic- and exponential-terms model has been selected to predict the SRP underground cable steady state rating.

5 SUMMARY AND CONCLUSION

This work makes three contributions. It develops an analytical approach to estimating cable ampacity. It uses CYMCAP to model many underground installations and estimate the cable ratings under steady-state and transient conditions. It develops a nonlinear model that can be used simply to predict steady state ampacity ratings.

In the first part of this work, an analytical approach for calculating cable steady state ratings was developed. The thermal circuit has been created to represent the cable component and surrounding environment (duct bank and native soil) as thermal resistances and the node potentials in the thermal circuit analogized the temperatures at each layer (see Fig. 2.9).Thus, the cable ampacity rating can be calculated by solving the potential and current in the thermal circuit. To take the cable mutual heating into account, the superposition was used. The analytical approach was applied to determine the steady state ampacity of the following scenario: flat arrangement, three single core cables.

In addition to analytical approach of cable rating calculation, the computational software CYMCAP was used to perform the numerical experiments. The input parameters such as the cable components, duct bank thermal resistivity, backfill thermal resistivity, load factors, and load curves (for transient calculation only) were gathered. Since the load factors in Papago Buttes-Scottsdale line and Beeline-Pico line are higher than the values that the SRP engineer expected, those load factors were re-calculated. After gathering and preparing the input parameters, the SRP 69 kV underground cable steady state and transient ampacities were calculated. Compared with the existing ratings, the new steady state ratings were very close to the existing ones. However, it can be seen

that in Table 3.3 the existing ratings were rounded to the nearest 25 amp increment or decrement. With the help of computational software CYMCAP, the cable ratings were generated without being rounded which means the updated ratings provide more accurate results.

To provide an alternative way to estimate the underground cable ratings, three regression models were generated. The regression models were built to find the relationship between the response variable (ampacity) and a set of related predictor variables. The predictor variables include the cable sizes, duct bank thermal resistivity, soil thermal resistivity, and cable depth. Residual plots which are one of most important diagnostic methods for model validation were generated to reveal how well the models explained the data. The residual plot of the mixed logarithmic/exponential model shows random pattern of residuals centered on zero. Of the three models investigated, this one appeared to perform the best.

REFERENCE

[1] F. Kiessling, P. Nefzger, J. F. Nolasco and U. Kaintzyk "Overhead Power lines: Planning, Design, Construction (Power Systems)" New York, Springer, 2003.

[2] G. J. Anders, *Rating of electric power cables: ampacity computations for transmission, distribution, and industrial application*, New York: IEEE Press Power Engineering Series, 1997.

[3] National Fire Protection Association (NFPA) 70, National Electrical Code, 1981.

[4] M.A. El-Kady, "Calculation of the sensitivity of power cable ampacity to variations of design and environmental parameters," IEEE Transaction on Power Apparatus and Systems, Vol. PAS-103, No. 8, 1984.

[5] H. Poritsky, "The field due to two equally charged parallel conducting cylinders,"Journal of Math, pp. 213-217, 1931.

[6] H. Goldenberg, "External thermal resistane of two buried cables. Restricted application of superposition," Pro. IEE, vol. 116, no. 5, pp. 822-826, 1969.

[7] J. H. Neher, "Procedures for calculating the temperature rise of pipe cable and buried cables for sinusoidal and rectangular loss cycles," AIEE transactions, Vol. 72, part 3, pp. 541-545, 1953.

[8] L. Heinhold, Power Cables and their Application, part 1, 3rd edition, Siemens Aktiengesellschaft, 1990.

[9] J. H. Neher, and M. H. McGrath, "The calculation of the temperature rise and load capability of cables systems," AIEE Transactions, Vol. 76, part 3, pp. 752-772, 1957.

[10] IEC 287, "Calculation of the continuous current rating of cables (100%) load factor," IEC Publication 287, 1982.

[11] City of Tempe, Arizona, http://www.tempe.gov/index.aspx?page=1195.

[12] D. C. Montgomery, Introduction to Linear Regression Analysis, 4th edition, John Wiley & Sons, Inc., 2006.

APPENDIX I

TRAINING DATASET

	x_1	x_2	x_3	x_4	y
1	1500	0.9	1	4	1666
2	1500	0.9	1	5	1638
3	1500	0.9	1	6	1616
4	2000	0.9	1	4	1892
5	2000	0.9	1	5	1860
6	2000	0.9	1	6	1834
7	1500	0.95	1	4	1658
8	1500	0.95	1	5	1630
9	1500	0.95	1	6	1608
10	2000	0.95	1	4	1882
11	2000	0.95	1	5	1852
12	2000	0.95	1	6	1826
13	1500	1.05	1	4	1640
14	1500	1.05	1	5	1614
15	1500	1.05	1	6	1594
16	2000	1.05	1	4	1862
17	2000	1.05	1	5	1832
18	2000	1.05	1	6	1808
19	1500	0.9	1.2	4	1600
20	1500	0.9	1.2	5	1572
21	1500	0.9	1.2	6	1546
22	2000	0.9	1.2	4	1816
23	2000	0.9	1.2	5	1782
24	2000	0.9	1.2	6	1754
25	1500	0.95	1.2	4	1594
26	1500	0.95	1.2	5	1564
27	1500	0.95	1.2	6	1540
28	2000	0.95	1.2	4	1808
29	2000	0.95	1.2	5	1774
30	2000	0.95	1.2	6	1746
31	1500	1.05	1.2	4	1578
32	1500	1.05	1.2	5	1550
33	1500	1.05	1.2	6	1528
34	2000	1.05	1.2	4	1790
35	2000	1.05	1.2	5	1758
36	2000	1.05	1.2	6	1730
37	1000	0.95	1.2	4	1304
38	1250	0.95	1.2	4	1468

39	1500	0.95	1.2	4	1594
40	1750	0.95	1.2	4	1704
41	2000	0.95	1.2	4	1808
42	2250	0.95	1.2	4	1878
43	2500	0.95	1.2	4	1950
44	2750	0.95	1.2	4	2022
45	1500	0.6	1.2	4	1650
46	1500	0.9	1.2	4	1600
47	1500	1.2	1.2	4	1556
48	1500	1.5	1.2	4	1516
49	1500	1.8	1.2	4	1478
50	1500	2.1	1.2	4	1442
51	1500	2.4	1.2	4	1410
52	1500	2.7	1.2	4	1378
53	1500	0.9	0.8	4	1740
54	1500	0.9	1.2	4	1600
55	1500	0.9	1.6	4	1492
56	1500	0.9	2	4	1400
57	1500	0.9	2.4	4	1326
58	1500	0.95	1.2	1	1740
59	1500	0.95	1.2	2	1676
60	1500	0.95	1.2	3	1630
61	1500	0.95	1.2	4	1594
62	1500	0.95	1.2	5	1564
63	1500	0.95	1.2	6	1540
64	1500	1.1	1.2	4	1478
65	1500	1.1	1.2	4.3	1442
66	1500	1.1	1.2	4.6	1410
67	1750	1.1	1.2	4.3	1740
68	1750	1.1	1.2	4.6	1600
69	2000	1.1	1.2	4.3	1740
70	2000	1.1	1.2	4.6	1630

APPENDIX II

VALIDATION DATASET

	x_1	x_2	x_3	x_4	y
1	1500	0.9	1	4.2	1660
2	1750	0.9	1	4.2	1776
3	2250	0.9	1	4.2	1960
4	2500	0.9	1	4.2	2034
5	1500	0.9	1	4.3	1658
6	2250	0.9	1	4.3	1956
7	2500	0.9	1	4.3	2032
8	2000	0.9	1	4.4	1878
9	2500	0.9	1	4.4	2028
10	1500	0.9	1	4.5	1652
11	1750	0.9	1	4.5	1768
12	2000	0.9	1	4.5	1876
13	2250	0.9	1	4.5	1950
14	1500	0.9	1	4.6	1648
15	1750	0.9	1	4.6	1764
16	2000	0.9	1	4.6	1872
17	2250	0.9	1	4.6	1946
18	1500	1	1	4.7	1630
19	1750	1	1	4.7	1744
20	2000	1	1.1	4.7	1812
21	2500	1	1.1	4.7	1954
22	1500	1	1.1	4.8	1594
23	2000	1	1.1	4.8	1808
24	2250	1	1.1	4.8	1878
25	2500	1	1.1	4.8	1950
26	1500	1	1.1	4.9	1592
27	1750	1	1.1	4.9	1702
28	2000	1	1.1	4.9	1806
29	2250	1	1.1	4.9	1876
30	1500	1	1.1	5	1588
31	2250	1	1.1	5	1872
32	2500	1	1.1	5	1944
33	1500	1	1.1	5.1	1586
34	1750	1	1.1	5.1	1698
35	2000	1	1.1	5.1	1800
36	2250	1	1.1	5.1	1870
37	2500	1	1.1	5.1	1940
38	1500	1	1.2	5.2	1552

39	1750	1	1.2	5.2	1660
40	2000	1	1.2	5.2	1760
41	2250	1	1.2	5.2	1828
42	2500	1	1.2	5.2	1896
43	1500	1.1	1.2	5.3	1536
44	2000	1.1	1.2	5.3	1742
45	2250	1.1	1.2	5.3	1808
46	2500	1.1	1.2	5.3	1876
47	1750	1.1	1.2	5.4	1640
48	2000	1.1	1.2	5.4	1738
49	2250	1.1	1.2	5.4	1806
50	2500	1.1	1.2	5.4	1874
51	1750	1.1	1.2	5.5	1638
52	2250	1.1	1.2	5.5	1802
53	2500	1.1	1.2	5.5	1870
54	1750	1.1	1.2	5.6	1636
55	2000	1.1	1.2	5.6	1734
56	2250	1.1	1.2	5.6	1800
57	2500	1.1	1.2	5.6	1868
58	1500	1.1	1.2	6	1520
59	1250	1.1	2.5	6	1150
60	1250	2.5	2.5	4	1238
61	2000	0.6	0.8	6	1990
62	1250	2	0.8	6	1410
63	2000	2	0.8	6	1634
64	1250	2.5	0.8	6	1334
65	2000	2	2	6	1414
66	2000	2.5	2	6	1360
67	1250	0.6	0.8	6	1516
68	1250	0.6	2.5	4	1352
69	1250	0.6	2	4	1524
70	2000	0.6	2	4	1880
71	2000	2	2	4	1612
72	1250	2.5	2	4	1238
73	2000	2.5	2	4	1514
74	2500	0.90	1.00	4.2	2034
75	2500	0.90	1.00	4.4	2028
76	2500	1.00	1.00	4.6	2000
77	2500	1.00	1.10	4.8	1950

78	2500	1.00	1.10	5.2	1944
79	2500	1.00	1.20	5.5	1896
80	2500	1.10	1.20	6	1870